

LB | DON | 66 | 2020

DEE 05/233 ✓

**EXPERIMENTAL STUDY ON  
BEHAVIOR OF MOV BASED SURGE ARRESTORS  
UNDER DISTORTED SUPPLY VOLTAGES**

I. P. S. Ilangakoon

159307P

**LIBRARY**  
UNIVERSITY OF MORATUWA, SRI LANKA  
MORATUWA

Thesis/Dissertation submitted in partial fulfillment of the requirements for the degree  
of Master of Science in Electrical Engineering


Department of Electrical Engineering

University of Moratuwa  
Sri Lanka

621.3 "2020"  
621.3(043)

March 2020

University of Moratuwa



TH4268

TH 4268

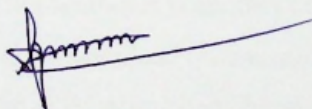
TH 4268 + CD ROM  
is not working

## DECLARATION

I declare that this is my own work and this thesis/dissertation does not incorporate without acknowledgment any material previously submitted for a Degree or Diploma in any other University or institute of higher learning and to the best of my knowledge and belief, it does not contain any material previously published or written by another person except where the acknowledgment is made in the text.

Also, I hereby grant to University of Moratuwa the non-exclusive right to reproduce and distribute my thesis/dissertation, in whole or in part in print, electronic or other medium. I retain the right to use this content in whole or part in future works (such as articles or books).

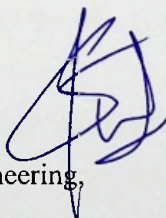
Signature of the Author:  
I. P. S. Ilangakoon



Date: 20/03/2020

The above candidate has carried out research for the Masters Dissertation under my supervision.

Signature of the supervisor:  
Dr. W. D. A. S. Rodrigo  
Senior Lecturer Grade I,  
Department of Electrical Engineering,  
University of Moratuwa,



Date: 20/03/2020



## **ABSTRACT**

Surges due to lightning and various switching operations are a common phenomenon in electrical power systems. Due to surges, there can be transient overvoltages in the lines as high as many times the normal supply voltage. Equipment connected to the line cannot withstand these high voltages since the internal circuitry has not been designed to withstand surges. Metal oxide Varistor (MOV) is one of the best clamping devices used for electronic equipment from surges. Metal Oxide Surge Arrestor (MOSA) is made by stacking several numbers of MOV blocks to match system voltages for power system applications. Throughout life, MOVs are exposed to system voltage stress endlessly. Thus, the stress these devices experience is comparatively higher especially in the case of MOSAs.

Supply voltage distortion due to harmonics is another common phenomenon found in power systems due to modern non-linear loads connected to power systems. This study is conducted to access the effect of supply voltage harmonics on the life expectancy of MOVs. Electrical and thermal experiments performed to validate relevant models for MOVs. Using simulations, and a life expectancy model, the effect of various cases of voltage distortion studied to find the effect on life expectancy.

Based on the above results, recommendations have been made on how to select maximum continuous voltage of surge arrestors to minimize the effect of supply voltage harmonics on life expectancy.

## ACKNOWLEDGEMENTS

First and foremost, I would like to express my sincere gratitude to my supervisor Dr. W. D. A. S. Rodrigo for his continuous guidance, constructive feedback and support extended throughout this research. Despite his busy schedule, he always remained accessible and his guidance and advice, expertise and insights were by all means truly invaluable.

The special attention paid by Dr. J.V.U.P Jayathunga on this research opened my eyes to different approaches to conduct the study. Comments made by her and the advice given made the study more meaningful.

It's with great pleasure that I thank Mrs. Sujani Madurapperuma, Electrical Engineer Meter Testing Laboratory DD2-Ceylon Electricity Board for her kind assistance in the successful completion of laboratory testing.

I. P. S. Ilangakoon

March 2020



## TABLE OF CONTENT

Declaration of the candidate & Supervisor.....	i
Abstract.....	ii
Acknowledgments.....	iii
Table of content.....	iv
List of Figures.....	vii
List of Tables.....	ix
List of Abbreviations.....	xi
1. Introduction.....	1
1.1 Introduction to MOVs.....	3
1.1.1 Physical Characteristics.....	3
1.1.2 Theory of Operation.....	5
1.1.3 Electrical Properties.....	6
1.1.4 Definitions.....	6
1.2 Research Motivation.....	7
1.3 Objectives.....	7
1.4 Methodology.....	8
1.5 Outline of the Thesis.....	9
2. LITERATURE REVIEW.....	10
2.1 Introduction.....	10
2.2 Continues Current Condition through MOV.....	10
2.3 Conclusions.....	15
3. Experimental Work.....	17
3.1 Introduction.....	17
3.2 Selection of Equipment.....	17
3.2.1 AC Voltage Source.....	17
3.2.2 DC Voltage Source.....	18

3.2.3	Measurement Equipment .....	18
3.3	MOV Samples .....	20
3.4	Leakage Current and Power Dissipation Measurement When Supply Voltage is Distorted .....	20
3.5	Power Dissipation vs Temperature Rise Measurement.....	22
4.	Simulation Studies .....	24
4.1	Introduction .....	24
4.2	MOV Modelling in Electrical Domain.....	24
4.2.1	MOV Model in MATLAB Simulink .....	24
4.2.2	Model Parameters [19].....	25
4.2.3	Modified MOV Model .....	26
4.2.4	Simulation and Results.....	27
4.2.5	Discussion .....	32
4.3	MOV Modelling in Thermal Domain (Steady State).....	34
4.3.1	ANSYS Simulation .....	34
4.3.2	Model Validation .....	36
4.3.3	Results and Discussion.....	37
5.	Estimation of effect of supply voltage distortion on lifeTime of MOV .....	39
5.1	Introduction .....	39
5.2	Lifetime Estimation Model .....	39
5.3	Results .....	40
5.4	Discussion .....	41
6.	Discussion.....	46
6.1	Introduction .....	46
6.2	Results in Contrast with Literature.....	46
6.3	Limitations and Applicability for Utility-Scale MV Applications.....	47





7. Conclusions and Recommendations .....	48
7.1 Recommendations .....	48
7.2 Study Limitations and Suggestions for Future Work.....	50
8. References.....	51
Appendix I: Results of the Electrical Experiments Performed.....	53
Appendix II: Results of the Simulations Performed.....	54
Appendix III: Measurements of MOV Voltage at 1mA DC Current.....	57
Appendix IV: Yokogawa WT310 Measurement Error Analysis.....	58

## List of Figures

Figure 1-1: Schematic representation of the microstructure of a MOV, grains of conducting ZnO (average-sized) are separated by intergranular boundaries [1] .....	4
Figure 1-2: Optical photomicrograph of a polished and etched section of a varistor [1] .....	4
Figure 1-3: MOV V-I Characteristics [1].....	6
Figure 2-1: V – I Characteristics of the ZnO block before and after degradation .....	11
Figure 3-1: Accuracy data. Yokogawa WT310 Power Meter.....	18
Figure 3-2: Measured Value (mA) vs Error ( $\mu$ A).....	19
Figure 3-3: Circuit Diagram of MOV Testing Experiment .....	21
Figure 3-4: Experimental Setup .....	21
Figure 3-5: Leakage Current Waveform for Distorted Supply Voltage of 230Vrms (Fundamental + 5 <sup>th</sup> Harmonic 20%).....	22
Figure 3-6: Temperature vs Power Dissipation .....	23
Figure 4-1: MOV Model in MATLAB Simulink. ....	24
Figure 4-2: MOV Equivalent Model.....	26
Figure 4-3: MOV Equivalent Circuit at Low Currents .....	27
Figure 4-4: MATLAB Simulation Model of MOV .....	27
Figure 4-5: Simulation Block Diagram in MATLAB Simulink.....	28
Figure 4-6: Applied Voltage ( $U_b$ ), Resistive Current Component through MOV ( $I_b$ : MOV nonlinear Resistance), Capacitive Current Component through MOV ( $I_b$ : MOV Capacitance), and Total Current through MOV ( $I_b$ : Series RLC Branch) .....	30
Figure 4-7: Applied Voltage ( $U_b$ ), Resistive Current Component through MOV ( $I_b$ : MOV nonlinear Resistance), Capacitive Current Component through MOV ( $I_b$ : MOV Capacitance), and Total Current through MOV ( $I_b$ : Series RLC Branch) .....	31
Figure 4-8: Leakage currents for different levels of distortion ( $I$ : Total leakage, $I_r$ : Resistive component and $I_c$ : Capacitive Component) .....	33
Figure 4-9: Cross Section of the Modelled MOV .....	34
Figure 4-10: Temperature Distribution of MOV Model in ANSYS.....	35
Figure 4-11: Simulated and Measured Surface Temperatures vs Heat Dissipation per Unit Volume.....	36



Figure 5-1: Per unit life expectancy with a peak value of Voltage waveform for different levels of distortion.....	41
Figure 5-2: Behavior of Peak Value of the waveform for different level of distortions for the same RMS value.....	42
Figure 5-3: Results for 8% THD in Voltage.....	44

## List of Tables

Table 1-1: IEEE-519-2014 Voltage Distortion Limits.....	2
Table 3-1: Ratings of the Selected MOV Samples .....	20
Table 3-2: Heat Dissipation and Temperature Rise Measurements of MOV Samples .....	22
Table 4-1: MOV Modelling Parameters .....	25
Table 4-2: Parameters Used During Simulation .....	26
Table 4-3: Harmonic Percentage Values and Phase Angles .....	29
Table 4-4: Simulation Measurements When Pure Sinusoidal Waveform Applied to MOV .....	31
Table 4-5: Simulation Measurements When 5 <sup>th</sup> Harmonic 20% Distorted Waveform Applied to MOV .....	32
Table 4-6: Simulated and measured temperature data .....	36
Table 5-1: Results of Lifetime Estimation for Different Levels of Distortion .....	40
Table 5-2: IEEE-519-2014 Voltage Distortion Limits.....	43
Table 5-3: Composition of Harmonics for 8% THD .....	43
Table 7-1: Recommended MCOV Values .....	49



## List of Abbreviations

Abbreviation	Description
CEB	Ceylon Electricity Board
MOV	Metal Oxide Varistor
IEC	International Electrotechnical Commission
R&D	Research and Development
SPD	Surge Protection Device
RMS	Root Mean Square
V	Voltage
I	Current
GDT	Gas Discharge Tubes
TOV	Temporary Overvoltage
TVS	Transient Voltage Suppression
PCC	Point of Common Coupling
MOSA	Metal Oxide Surge Arrestor
LV	Low Voltage
HV	High Voltage
MV	Medium Voltage
MCOV	Maximum Continuous Operating Voltage
IEEEE	Institute of Electrical and Electronic Engineers
AC	Alternating Current
DC	Direct Current
TSC	Thermally Stimulated Current
THC	Third Harmonic Component
MSCM	Modified Shifted Current Method
RMS	Root Mean Square

### 1. INTRODUCTION

Metal Oxide Varistor (MOV) is the proven most popular building block of transient overvoltage protection devices used for decades in power systems and electrical/electronic appliances. Nonlinear V-I characteristics, fast response and high transient energy absorption capacity of MOVs are the prominent characteristics as a building block candidate for transient overvoltage protection devices. In literature, transient overvoltage protection devices are identified as Surge Protection Devices (SPDs), Lightning Arrestors and Surge Arrestors. MOV is the basic building block for many of these devices. Some types of devices contain transient overvoltage protection devices like Gas Discharge Tubes (GDT) or Transient Voltage Suppression (TVS) Diodes together with MOVs. The surge arrestors made of MOVs are identified as Metal Oxide Surge Arrestors (MOSA)

Throughout the service life, the Surge Protection Devices (SPDs) made of MOVs are exposed to the system voltage. As an example, in a 400v Ac system, MOV connected between neutral and a phase will be exposed to a 230Vrms voltage waveform throughout the service life. SPD will conduct very small leakage current (in the order of 30 – 300 micro Amperes) at the rated voltage of the system. If transient overvoltages are present, MOV starts to conduct and maintain the voltage at a guaranteed level up to its capability limits.

Supply voltage distortion is an inevitable factor in power systems [10, 11]. Distortion occurs due to the association of nonlinear loads to the system. Nonlinear loads have become a reason for nonlinear voltage drops across the impedance of power system components and hence system voltage gets distorted in the power system. IEEE-519-2014 standard [2] has laid maximum values for the possible distortion at the Point of Common Coupling (PCC). Values are given the table below (Table 1-1)



**Table 1-1: IEEE-519-2014 Voltage Distortion Limits**

**Table 1—Voltage distortion limits**

Bus voltage $V$ at PCC	Individual harmonic (%)	Total harmonic distortion THD (%)
$V \leq 1.0 \text{ kV}$	5.0	8.0
$1 \text{ kV} < V \leq 69 \text{ kV}$	3.0	5.0
$69 \text{ kV} < V \leq 161 \text{ kV}$	1.5	2.5
$161 \text{ kV} < V$	1.0	1.5 <sup>a</sup>

<sup>a</sup>High-voltage systems can have up to 2.0% THD where the cause is an HVDC terminal whose effects will have attenuated at points in the network where future users may be connected.

Source: IEEE 519-2014 - IEEE Recommended Practice and Requirements for Harmonic Control in Electric Power Systems.

Stable operation of MOVs is a critical factor for the safe operation of protected downstream systems. The stability refers to as the operation of MOV within the expected  $V - I$  characteristic limits. Environmental conditions, as well as the characteristics of the supply voltage they are exposed to [18], are the factors for loss of stability. The loss of stability is identified as the failure is referred to as the MOV failure [15, 16]. MOVs fail catastrophically followed by the loss of stability due to the excess heat generated inside the MOV. In the literature electrical degradation of MOVs has been identified due to two factors namely exposure to AC or DC voltages for a prolonged period [3,12] and due to surge currents discharged through the MOV [13, 14]. Quantification of degradation is done by measuring the increment in the clamping voltage.

Under this research work, the relationship of the supply voltage distortion with the behavior of MOVs is studied under rated voltage conditions. Different levels of voltage distortions are generated and applied to a set of samples of MOVs and the change in the leakage current is investigated. Higher leakage current is a sign of failure in the MOV. There will be a high level of power dissipation as well and hence a

temperature rise. This extra stress will degrade the MOV and it becomes a cause for eventual thermal run off of the MOV.

## **1.1 Introduction to MOVs**

Metal Oxide Varistors are nonlinear resistors which exhibit electrical properties equivalent to back to back Zener diodes. The main materials MOVs are made of are metal oxides such as Zinc, Bismuth, and Manganese. A ceramic semiconductor is made by sintering the metal oxide during the manufacturing process. The microstructure made during the process is crystalline and hence the MOV is inherited the capability of dissipating huge amounts of energy in transients. This is the reason why MOVs are the application for suppression of high energy transients occurring in electrical power systems and electronic circuits. The shape of the MOVs can be different due to the flexibility of the manufacturing process. The disk shape with leads radial is the shape found commonly.

### **1.1.1 Physical Characteristics**

The transients in the power systems can be categorized as external transients and internal transients. External transients are essentially lightning while internal transients are occurring due to the following reasons.

1. Switching relays
2. Switching inductive loads
3. Discharging capacitors

MOVs are used to protect electronic circuits from both of the above types of transients and MOV is used as a building block for making MOSAs that are used in power system applications. Typical current ratings are from 20A to 500A while the energy ratings are between 0.05J to 2.5J[1]

The varistor core is made of ZnO semiconductor grains. Their average size "d" is shown in the model in figure 1-1 below. The resistivity of ZnO is less than  $0.3 \Omega\text{-cm}$  [1].



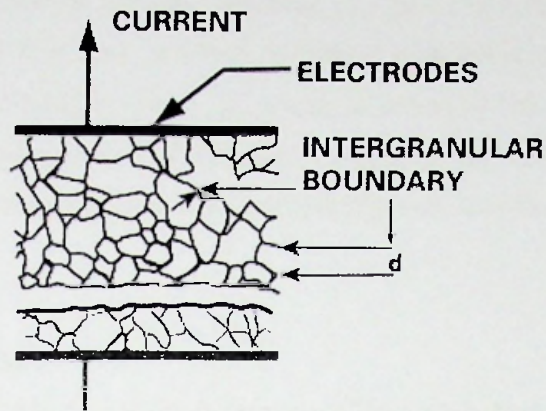


**Figure 1-1: Schematic representation of the microstructure of a MOV, grains of conducting ZnO (average-sized) are separated by intergranular boundaries [1]**

A cross-section of the material is shown in Figure 1-2, which illustrates the ceramic microstructure [1]. Each ZnO grain of the ceramic acts like a semiconductor junction at the grain boundary [1].

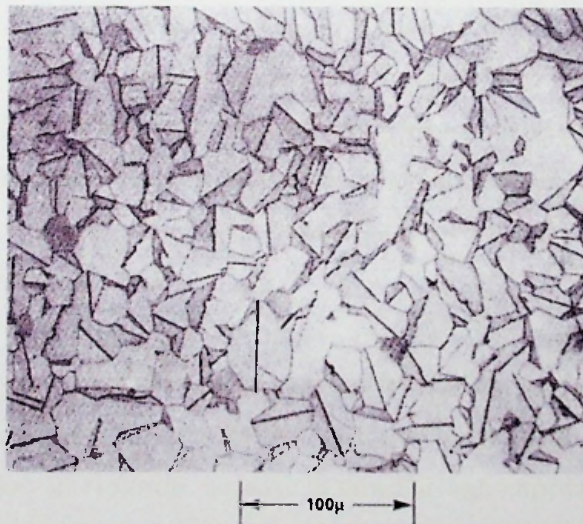


**Figure 1-2: Optical photomicrograph of a polished and etched section of a varistor [1]**

Varistors are fabricated by forming and sintering Zinc Oxide-based powders into ceramic parts [21]. These parts are then electroded with either thick film Silver or arc/flame sprayed metal [21]. Since the nonlinear electrical behavior occurs at the boundary of each semiconducting ZnO grain, the varistor can be considered a "multi-junction" device composed of many series and parallel connections of grain boundaries [1].

### 1.1.2 Theory of Operation

The internal core structure of MOV is polycrystalline, hence their characteristics are different and complex in comparison to traditional semiconductors. Using sensitive measurement equipment, the characterization of the Voltage and current behavior of MOVs has been performed to a certain extent. Manufacturers are still working to better understand the characteristics beyond today's knowledge. Understanding the electronic phenomena taking place between grain borders, or junctions between the ZnO grains is the basis for understanding the characteristics of MOVs.

One of the theories proposed that electronic tunneling happened via an insulating second phase layer at the grain boundaries. A series and parallel assembly of semiconductor diodes is a better model proposed which matches best with varistor characteristics. Grain boundaries in this model consists of defect states trapping free electrons from n-type ZnO grains. They form a layer of charge depletion in the nearby area to the grain boundaries.[1]

1000 Angstrom is the measured average value of the depletion layer calculated. Other model are proposing single-junction operations. Depletion layers in the single-junction model block the flow of electrons. because of this, the high impedance characteristics at low voltage are attributed. Under low voltage conditions, a leakage current flows which is due to the free flow of electrons through the grain boundaries. This current is sensitive to the temperature.[1]



### 1.1.3 Electrical Properties

Typical V-I Characteristics of a MOV is shown in the figure below figure 1-3. These nonlinear characteristics can be divided into 3 regions [1].

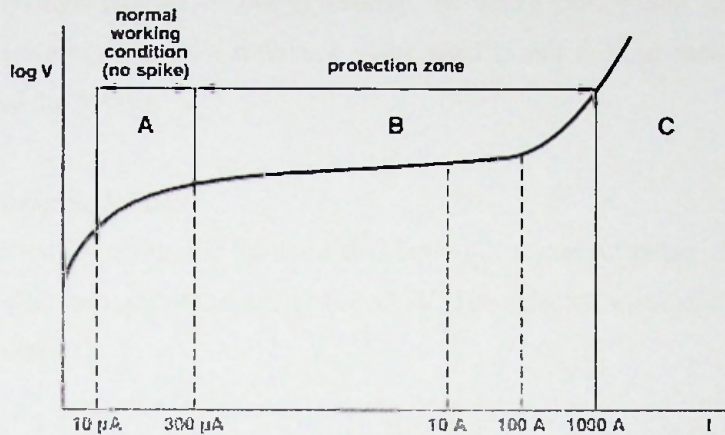


Figure 1-3: MOV V-I Characteristics [1]

**Region A:** Normal working zone: Current between  $10 \mu\text{A}$  to  $300 \mu\text{A}$  [1].

**Region B:** Protection (clamping) Region: Voltage is kept nearly constant protecting to downstream [1].

**Region C:** Maximum surge current: The maximum peak current that the varistor can withstand (only) once in its lifetime [1].

### 1.1.4 Definitions

#### Maximum Continuous Voltage:

The maximum value of the voltage which may be applied continuously between the terminals of the MOV. For all types of AC voltages, the voltage level determination is given by the crest voltage  $\times 0.707$  [1].

**Voltage at 1mA or Varistor Voltage ( $V_{1mA}$ ):**

When the DC voltage is adjusted so that a current of 1mA is flowing through the MOV, the corresponding value of the voltage is taken as  $V_{1mA}$ . At 1mA MOV dissipates a comparatively high amount of power making the MOV hot, which can make the measurement wrong.  $V_{1mA}$  is a reference value used in not only in modeling but in comparison of the MOVs.

**Maximum Clamping Voltage**

This is measured following the standard IEC 60060-2. A current pulse of 8  $\mu$ s/20  $\mu$ s (rising time/ decreasing time) is sent to the MOV. The selected value of the current is the class current. [1]

**Maximum Non-Repetitive Surge Current**

The shape of the pulse, number of pulses and duty cycle of the pulse are the factors that determine the maximum surge current allowed through the device. The maximum non-repetitive surge current is a characterization parameter which demonstrate the capability of the MOV in withstanding surge currents. Beyond this current, MOV will experience catastrophic failure, which needs to be avoided using a series fuse of suitable rating. [1]

**1.2 Research Motivation**

An incident has been found in a scrap metal melting factory in Sri Lanka, where an induction furnace is operated for melting scrap metal. Frequent failure of surge arrestors in this location is reported. The level of voltage distortion at the installation is about 5 – 10% (at 33kV level measured through a voltage transformer). Therefore, it is suspected that the level of voltage distortion has a relationship with the premature failure of surge arrestors.

**1.3 Objectives**

The main objective of this study was to find out the effect of supply voltage harmonics on the lifetime of the MOV type surge arrestors. Sub objectives are:



1. Studying the leakage current behavior of MOVs under different levels of supply voltage distortion due to harmonics.
2. Proposing methods/remedies for selecting suitable surge arrestors for harmonic rich environments if voltage harmonics cause problems to the MOVs.

#### **1.4 Methodology**

A representative batch of MOVs is selected to conduct the experiments. Using a suitable voltage source, distorted waveforms are generated by varying harmonic orders, amplitudes and phase angles. These voltages are fed into the selected MOVs and leakage current is measured using a suitable measurement equipment. Then the MOV is modeled in MATLAB Simulink and the model is tuned to match with the measurement data.

In the next experiment, the same MOV samples are fed with DC voltages and the surface temperature rise is measured against the different power dissipation levels. ANSYS is used to model the MOV thermally and the model is tuned to match with the results of the experiment.

Using electrical model, different levels of distortions are simulated with the MOV model and power dissipation, leakage current values are obtained. Then the power dissipation values are fed to the thermal model to estimate the possible temperature rise of the MOV. Using literature, the effect on MOV lifetime is estimated due to the rise of the temperature.

Finally, the maximum allowed distortion levels described in the IEEE-519-2014 standard are taken into consideration to and the possible maximum effect on lifetime is calculated. Based on these findings, recommendations are made as remedial actions to the existing selection criteria of maximum continuous operating voltage of surge arrestors.

## **1.5 Outline of the Thesis**

Chapter 2 is the literature study conducted which describes the related work carried out prior. Furthermore, it identifies the research gap between the proposed work and literature.

Chapter 3 describes the thermal and electrical experiments performed on selected MOV samples. Further, it describes the equipment used for measurement and voltage sources.

Chapter 4 is focused on the simulation studies. The first part contains the electrical domain modeling conducted using MATLAB while the latter part is about the thermal domain modeling conducted in ANSYS.

Chapter 5 describes the lifetime estimation model. Using this model together with thermal and electrical models, lifetime estimation is done for various scenarios.

Chapter 6 is a discussion about the overall work carried out under this research.

Chapter 7 presents the conclusions made based on the findings of chapter 5. Further, the recommendations made based on the findings are presented.



---

## 2. LITERATURE REVIEW

### 2.1 Introduction

In this section, the literature on the operating principles of MOVs and their interaction with system voltage is discussed. The focus is kept on the behavior of MOVs under system rated voltage but not due to surges under the scope of this work. Under these conditions, instead of high current short period surges, continuous current condition is experienced for a prolonged period which degrades the MOV eventually.

### 2.2 Continuous Current Condition through MOV

When in operation, a continuous leakage current is conducted through the MOV. Generally, this current is in the range of 10  $\mu\text{A}$  to 300  $\mu\text{A}$  in a healthy MOV. In the case of AC, this leakage current is comprised of two components namely resistive component and capacitive component. The higher the resistive current, and the period of exposure, the greater the effect on MOV's life expectancy.

The following studies have described the degradation of MOVs when exposed to dc or 50Hz sinusoidal waveforms of voltage.

1. In their work, Eda, Iga, and Matusoka [3] used 14mm diameter 1.8mm thick ZnO blocks to study the effect of DC and AC voltage bias and temperature bias on the thermal runaway of MOVs. They used a constant current DC supply to measure the V-I characteristic curves. A capacitance bridge is used to measure the capacitance and dielectric properties at 1Vrms in the frequency range of 500Hz to 1MHz. With no bias voltage applied, the thermally stimulated current (TSC) measurement is done in a quartz tube by changing the ambient temperature at a rate of 0.333 °K/s. They found that the V -I characteristics of ZnO changed after applying DC and AC bias due to the deformation of the Schottky barrier.

The finding of this works suggests that both ac and dc leakage current can drive the arrester to its end of life. The operating temperature is found to be a major influencing factor for the expected life of the ZnO.

- Zhou, Zhang, and Gong [4] worked on the degradation of low voltage ZnO MOVs caused by long time dc biasing based on the V - I characteristic tracing. At an environmental temperature of 140°C, a DC bias of 0.75  $V_{I_{ma}}$  is applied to ZnO blocks up to 120 hours. After this treatment, the V-I curve of the ZnO block is traced and compared with the original curve. One of the results obtained is shown in figure 2-1 below.

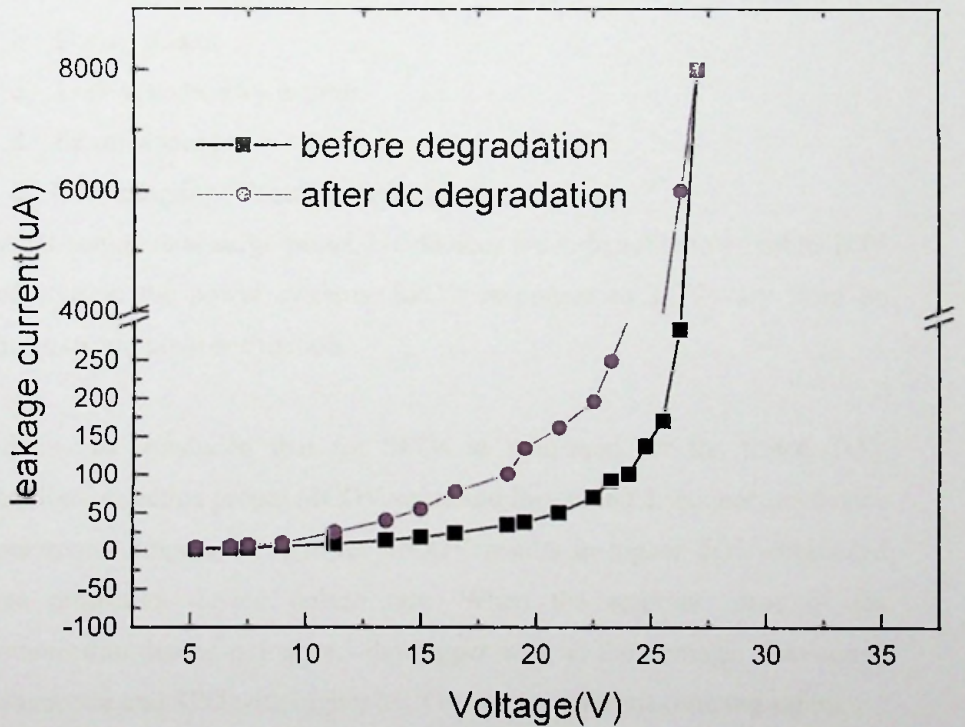


Figure 2-1: V - I Characteristics of the ZnO block before and after degradation



The results of this study suggest that due to the long time DC bias. The leakage current increases significantly as shown in figure 2-1. Further, they have found that breakdown voltage decreased after the degradation.

3. D. Kladar, F. Martzloff and D. Natasi [5] have discussed Temporary Over Voltage (TOV) effects on surge-protective devices. Though the SPDs can protect downstream systems from surges, their behavior of protection against the TOV (Temporary Over Voltage) is weak. Most of the situations, MOV will be the victim. This work reports TOV susceptibility tests on SPDs.

Authors have applied the following situation equivalent stress levels to MOVs and studied failures.

- a. Poor Voltage regulation
- b. During a fault
- c. Loss of secondary neutral
- d. Ferroresonance
- e. Commingling (Contact to HV circuits)

Typical commercial surge-protective devices are vulnerable to possible TOV conditions in the power systems. SPD's responses to TOV vary from no damage to complete destruction.

Authors has concluded that for SPDs to withstand for the tested TOV conditions, selecting proper MCOV value and fast-acting disconnection device is paramount important. A lower MCOV results in higher TOV originated surge protection device failure rate. When the response time of the disconnection device is longer, the bigger will be the damage. Fast-acting disconnecter and SPD with higher MCOV required for maximizing safety.

4. In this paper, Yuanfang Wen and Chengke Zhou [6] presents a methodology for predicting the lifetime of metal-oxide varistor which is widely used as a protective device in electrical and electronic transient overvoltage protection. The methodology followed in this research is based on the characteristic time-

current curve which is determined using the characteristic currents obtained from several stressed aging experiments. Results have shown that the proposed method is more effective and reliable than previously used methods.

Aging tests for MOV life prediction categorized into either U method or T method. The so-called U method is to test MOV with the temperature kept constant and voltage being varied to find the characteristic point in  $I(t)$  in time  $t_0$  while the T method is to keep the applied voltage as a constant and to vary the operating temperature. The envelope or critical point (point at which failure start) of  $I(t)$  curve of the U and T methods are plotted by doing a large number of experiments. By curve fitting to the envelope curve, authors have predicted lifetime of MOV under different voltage and temperature conditions.

This method is an experiment intensive method. Therefore, to practically apply to a particular MOV type, it is needed to estimate parameters by using experiments. Therefore, this method is not user-friendly.

5. Jaroszewski, Kostyla, and Wieczorek [7] simulated MOV in MATLAB. They tried to study the effect of the presence of harmonics in the supply voltage towards the leakage current based diagnosis techniques used for HV arrestors. Usually, the harmonic presence of leakage current is used to estimate the level of degradation which is correct for pure sinusoidal voltage supplied. Using the MOV model available in MATLAB, by adding a capacitor in series they performed several numbers of simulations. The findings are listed below.
  - a. The third harmonic current is significantly increased when harmonics are present in the supply voltage.
  - b. The appearance of the third harmonic current can be due to the operation of MOV beyond its MCOV.
  - c. The presence of harmonics in the supply voltage can cause misdiagnosis. Therefore, the presence of the harmonics in the supply shall be studied before making conclusions.



This work reveals that the THC can't be utilized for condition monitoring and performance analysis assessment of MOV arrestors operating under distorted supply voltages. This work has no attempt taken to quantify the effect of the presence of harmonics towards misdiagnosis or a method to do a compensation to the diagnosis when the supply voltage is distorted.

Another important finding is that the high current conduction through varistor devices results from operation voltage higher than rated MCOV. High current is a cause for the thermal run off of MOV.

6. MOV's leakage current is essentially comprised of two components namely resistive and capacitive current components which are orthogonal. Measuring the leakage current is useless for arrestor diagnosis unless the magnitude of the resistive component is extracted. If the supply voltage waveform is known, the resistive component can be extracted easily. Unfortunately, there for MV and HV arrestor diagnosis, there is no way to measure the voltage waveform. As a solution to this, Abdul-Malek, Yusof and Yousof [7] proposed the modified shifted current method (MSCM) algorithm, to extract the resistive current component from the measured total leakage current of MOV arresters. By adding a quarter cycle shifted leakage current to the original leakage current waveform, the resistive component can be subtracted from the waveform and thereby the capacitive component can be extracted. By experimenting with a real arrestor, the proposed scheme has been verified.

This technique is useful in situations where voltage waveform cannot be measured (HV installations). In such situations, by analyzing the leakage current waveform, it is possible to decompose the resistive and capacitive current components. The resistive current component is the indicator of the arrestor condition. However, by deeply studying the algorithm of MSCM, it is found that this technique is valid only when the supply voltage waveform is

sinusoidal. Therefore, this method is not applicable for condition monitoring of arrestors attached to power systems having distorted voltage sources.

### 2.3 Conclusions

Failure of MOSA/MOV can be due to two reasons. The first and most popular is the conduction of high surge currents through the device. These currents are in the range of few to few tens of kilo Amperes. If the current is above the maximum permitted surge current, MOV will fail in the first occurrence of the surge. When the current is less than the maximum permitted surge current, MOV will perform its duty by clamping the surge voltage to an acceptable value. MOV degrades at each surge current conduction. Leakage current through the MOV at power frequency voltage will be increased thereafter and the clamping voltage of the MOV will be increased. This will result in a decreased level of guaranteed protection to the downstream systems and eventual thermal runaway of MOV.

The second way is the continuous current condition through MOV at power frequency voltage due to long-term continuous exposure to ac or dc voltages. Shift of the V – I characteristics, increased leakage current, etc. are the symptoms of failures. The phenomena found in the literature which can cause MOVs to fail due to long term conduction are listed below.

- f. Poor Voltage regulation
- g. During a fault
- h. Loss of secondary neutral
- i. Ferroresonance
- j. Commingling (Contact to HV circuits)

Studies have been conducted to evaluate the effects of the above phenomena and found that the response varies from damage to destruction. The response can be diverse due to different brands, MCOV, and clamping voltage levels.

At present, the magnitude and spectral composition of leakage current is used as an indicator for the diagnosis of surge arrestors. The validity of these techniques in environments with distorted supply voltages is questionable. Therefore, a need is



found in the knowledge, on a technique to access the life expectancy of MOVs working in harmonic rich environments for prolonged periods. Therefore, a research avenue is found to study the effect of harmonic related overvoltage on the life expectancy of MOVs.

### 3. EXPERIMENTAL WORK

#### 3.1 Introduction

This chapter describes the experiments conducted to measure leakage currents of selected MOV samples under distorted and pure supply voltage conditions. The selection of voltage sources, measurement equipment, and environmental conditions are described as well.

#### 3.2 Selection of Equipment

##### 3.2.1 AC Voltage Source

The purpose of this study demands to measure the leakage currents of MOV samples under distorted supply voltages. For this purpose, it is required to generate waveforms with a controlled amount of distortion by superimposing a known number of harmonics with different levels of magnitude and phase angles.

The first approach was to use a function generator available. The main problem found is, function generator was its peak to peak amplitude limitation in addition to the limitation of the control of waveform shape. The solution found is the voltage source available inside the meter testing bench used for testing energy meters. This source allows the generation of waveforms with a known amount of distortion at a fixed RMS value. Details of the source is given below.

Make: ASTeL

Model: VIS-400

Output Voltage Range: 30Vrms -350V RMS

Harmonics Generation: Programmable

Output Frequency Range: 50 Hz to 2500Hz



### 3.2.2 DC Voltage Source

A DC voltage source is used to take the temperature measurements of MOVs concerning the leakage current through the MOV. The relationship between the internal power dissipation and surface temperature rise is developed using these measurements. Details of the source is given below.

Make: Ametek California Instruments

Model: 1501IX

Output DC Voltage Range: 0 – 400V

Resolution: 1V

Frequency Range: 16 - 1000Hz

Accuracy: 0.025%

Voltage Accuracy: 0.1% FS

Current Accuracy: 0.5% FS

### 3.2.3 Measurement Equipment

Yokogawa WT310 power analyzer is used as the measurement equipment. It can measure the RMS value of the leakage current upto of micro Amperes. Additionally, through the computer interface, the voltage and the current waveforms can be visualized. Up to 50<sup>th</sup>, harmonics can be measured in both voltage and current waveforms.

	WT310,WT330 (Voltage/Current)	WT310HC (Voltage, Current EXT sensor input)	WT310HC (Current Direct input)
DC	±(0.1% of reading +0.2% of range)	±(0.1% of reading +0.2% of range)	±(0.2% of reading +0.2% of range)
0.5Hz ≤ f < 45Hz	±(0.1% of reading +0.2% of range)	±(0.1% of reading +0.2% of range)	±(0.1% of reading +0.2% of range)
45Hz ≤ f ≤ 66Hz	±(0.1% of reading +0.1 % of range)	±(0.1% of reading +0.1 % of range)	±(0.1% of reading +0.1 % of range)
66Hz < f ≤ 1kHz	±(0.1% of reading +0.2 % of range)	±(0.1% of reading +0.2 % of range)	±(0.1% of reading +0.2 % of range)
1kHz < f ≤ 10kHz	±((0.07×f)% of reading +0.3 % of range)	±((0.07×f)% of reading +0.3 % of range)	±((0.13×f)% of reading +0.3 % of range)
10kHz < f ≤ 20kHz			±((0.13×f)% of reading +0.5 % of range)
10kHz < f ≤ 100kHz	±(0.5 % of reading +0.5 % of range) ±((0.04×(f-10))% of reading	±(0.5 % of reading +0.5 % of range) ±((0.04×(f-10))% of reading	

Figure 3-1: Accuracy data. Yokogawa WT310 Power Meter

Using the table above, the maximum possible error is calculated for the measurement range current 0 to 5mA and voltage 0 to 300V. The results are given in the figure 3-2 below (details available in Appendix IV).

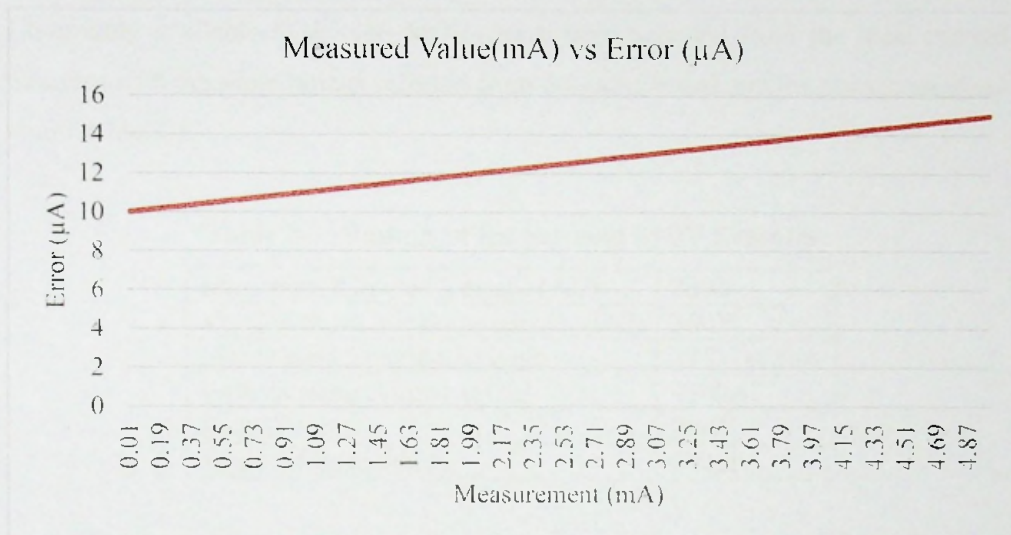


**Figure 3-2: Measured Value (mA) vs Error (µA)**

The typical leakage current of MOV is in the range of 30 to 300 µA. During the experiments, it is expected to measure currents in the range of 100 to 1000 µA. The maximum possible error within this range is 12 µA. Therefore, this equipment is considered suitable for taking measurements.

To take temperature measurements, a digital thermos meter with k type thermos couple is used. Details are given below.

Make: Omega

Model: HH506RA

Minimum Temperature Measurement: Type K -200°C (-328°F) J -210°C (-346°F) T -200°C (-328°F) E -210°C (-346°F) R 0°C (32°F) S 0°C (32°F) N -50°C (-58°F)

Maximum Temperature Measurement: Type K 1372°C (2501°F) J 1200°C (2192°F) T 400°C (752°F) E 1000°C (1832°F) R 1767°C (3212°F) S 1767°C (3212°F) N 1300°C (2372°F)





Resolution: 0.1 °C

Accuracy: K/J/T/E Type:  $\pm(0.05\% \text{ reading} + 0.3^\circ\text{C})$  on -50 to 1370°C

### 3.3 MOV Samples

Commonly available Disk type MOVs have been selected from the local market. Samples with the same ratings selected from the same brand and the ratings are given below table 3-1.

**Table 3-1: Ratings of the Selected MOV Samples**

Maximum Allowed Voltage (AC)	230V
Voltage at 1mA leakage current (DC)	360V
Maximum Clamping Voltage	595V at 50A
Withstanding Surge Current	4500A
Rated Power	0.6W
Typical Capacitance	560pf

### 3.4 Leakage Current and Power Dissipation Measurement When Supply Voltage is Distorted

This experiment is performed on three samples from the above-selected MOVs. MOV was mounted on an energy meter enclosure so that it could be easily mounted on the meter testing bench. Yokogawa power analyzer was connected appropriately for measuring the voltage across MOV and the current flowing through the MOV. The software package WT Viewer is used to acquire the data to a PC.

The circuit arrangement of the experimental setup is shown below.

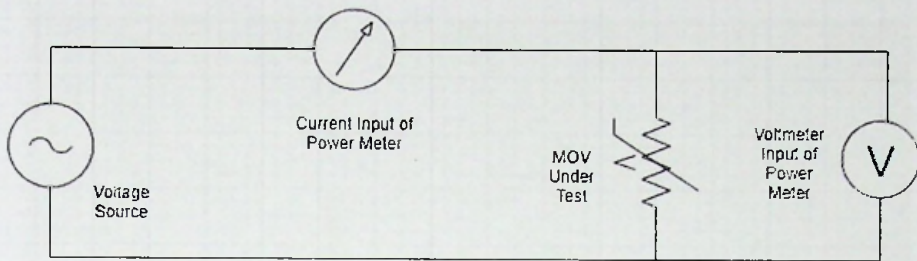


**Figure 3-3: Circuit Diagram of MOV Testing Experiment**

The photograph of the experimental setup is shown below as figure 3-4. The power meter and MOV under test are visible. The voltage source is not visible since it is an integral part of the meter testing bench,

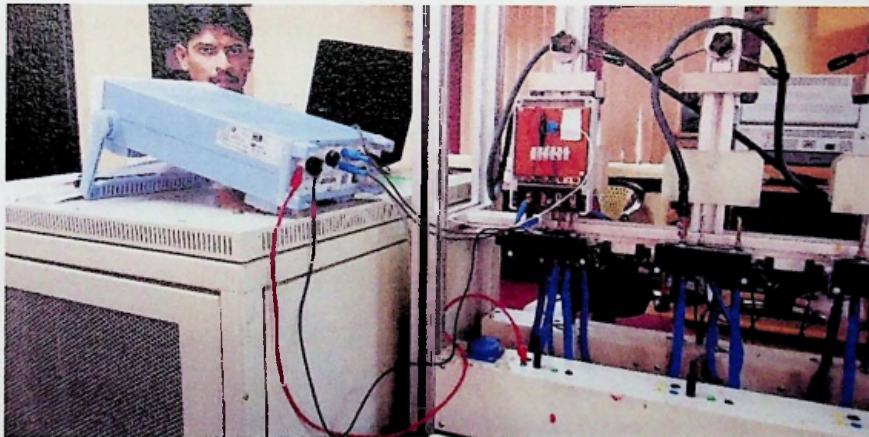


**Figure 3-4: Experimental Setup**

Using the computer interface of the voltage source control software, different waveforms created keeping the RMS value of the voltage at 230V. The experiment started with a pure sinusoidal voltage output. Harmonics were added gradually for a certain number of situations (assumed to be occurring in power systems). The waveform of one of the tested cases is shown below figure 3-5.



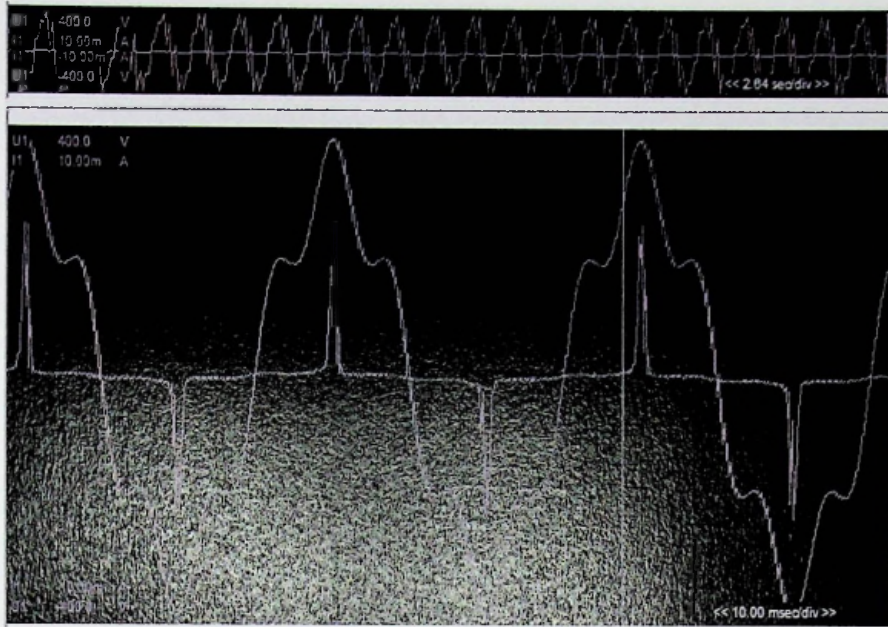


**Figure 3-5: Leakage Current Waveform for Distorted Supply Voltage of 230Vrms (Fundamental + 5<sup>th</sup> Harmonic 20%)**

Details of all experiments performed are shown in Appendix 1.

### 3.5 Power Dissipation vs Temperature Rise Measurement

Under this experiment, a DC source is utilized to supply MOV with a DC voltage. Calculated power dissipation and temperature rise measurements are noted down. Experiment was conducted inside a laboratory having a controlled temperature of 25°C. The voltage across the MOV is varied from 0 to its  $V_{1mA}$  (V). The collected measurements of the experiment is shown below table 3-2.

**Table 3-2: Heat Dissipation and Temperature Rise Measurements of MOV Samples**

Dissipation in Watts	Temperature Rise in °C		
	Sample 1	Sample 2	Sample 3
0.373	34.8	35.1	34.8
0.323	33.5	33.1	33.3

0.273	32.5	32.5	32.5
0.223	30.9	31.2	31.0
0.173	29.5	29.5	29.5
0.123	28.4	28.7	28.6
0.073	26.9	26.9	26.9
0.023	25.6	25.3	25.5
0	25.0	25.0	25.0

At  $V_{1mA}$ , MOV exhibited a surface temperature rise close to  $10^{\circ}\text{C}$  and proportional temperature rise for power dissipation values in between. These experiments give clear evidence of the linear relationship between the power dissipation and the temperature rise of the MOV. The relationship of temperature rise against the current and voltage are non-linear due to the nonlinear relationship between voltage and current behavior. Therefore, it is convenient to use the relationship of temperature rise against the power dissipation for the scope of this study. The above data is shown on the chart below figure 3-6 which explains the linear relationship.

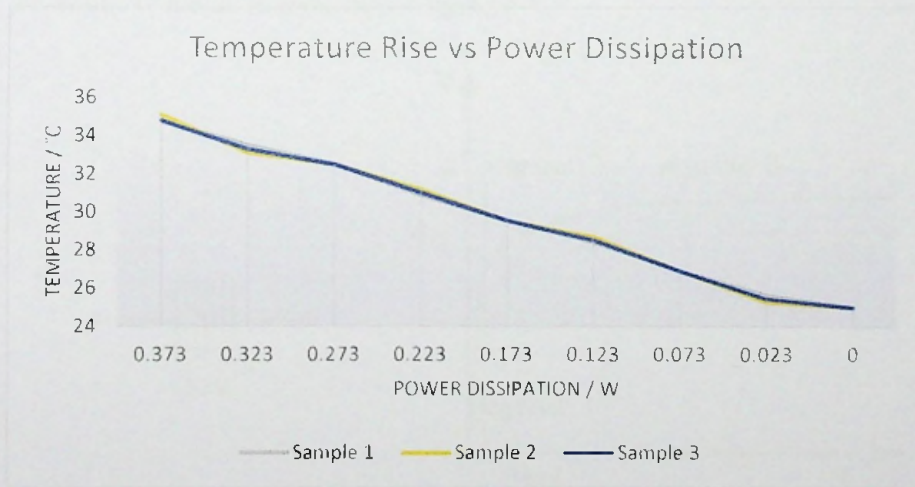


**Figure 3-6: Temperature vs Power Dissipation**



## 4. SIMULATION STUDIES

## 4.1 Introduction

This chapter describes the corresponding simulations done for the selected model of MOV samples. MATLAB Simulink software is used for the electrical domain simulation of MOVs. The thermal modeling of MOVs is done using the ANSYS software. The models used are tuned and modified to match with the MOV samples. Using simulation models, different scenarios of voltage distortion studied.

## 4.2 MOV Modelling in Electrical Domain

## 4.2.1 MOV Model in MATLAB Simulink

There is a block available for MOV in MATLAB Simulink platform [19]. Details of the available model is given below figure 4-1.

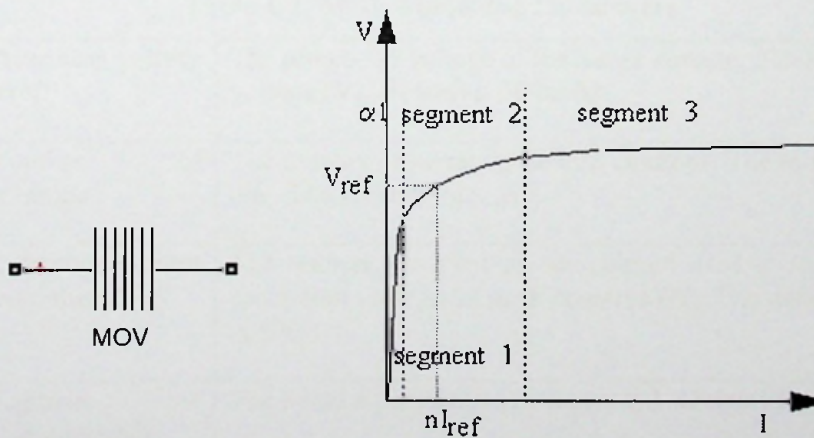


Figure 4-1: MOV Model in MATLAB Simulink.

The MOV model in Matlab implements a nonlinear resistor having similar characteristics to MOVs discs used for protecting power equipment from transient overvoltages. Multiple of MOV blocks are cascaded for high voltage applications

while series combinations used to dissipate more power from transients. The nonlinear V-I characteristic of each MOV column of the protection device is modeled by a combination of three exponential functions of the following form [19].

$$\frac{V}{V_{ref}} = k_i \left( \frac{I}{I_{ref}} \right)^{\frac{1}{\alpha_i}}$$

$$i = 1,2,3$$

V = Voltage

V<sub>ref</sub> = Reference Voltage

I = Current

I<sub>ref</sub> = Reference Current

k<sub>i</sub> = Proportionality Constant of segment i

1/α<sub>i</sub> = Tangent of angle curve deviating from the horizontal of segment i

#### 4.2.2 Model Parameters [19]

**Table 4-1: MOV Modelling Parameters**

1	Protection voltage V <sub>ref</sub> :	The protection voltage of the Surge Arrester block, in peak voltage (V). Default is 500e+03.
2	Number of columns	The number of metal-oxide disc columns. The minimum is one. The default value is 2.
3	Reference current per column I <sub>ref</sub>	The reference current of one column used to specify the protection voltage, in peak amperes (A). The default value is 500.
4	Segment characteristics 1	The k and α parameters of segment 1. Default is [.955 50].
5	Segment characteristics 2	The k and α parameters of segment 2. Default is [1.0 25].
6	Segment characteristics 3	The k and α characteristics of segment 3. Default is [.9915 16.5].





To simulate a single MOV, the following parameter values used

**Table 4-2: Parameters Used During Simulation**

	Parameter	Value	Notes
1	Protection voltage Vref:	360V	Measured DC voltage when the current through the MOV is 1mA (Appendix III)
2	Number of columns	1	To simulate 1 MOV disc
3	Reference current per column Iref	1mA	
4	Segment 1 characteristics	[.955 50]	Default values used
5	Segment 2 characteristics	[1.0 25]	Default values used
6	Segment 3 characteristics	[.9915 16.5]	Default values used

#### 4.2.3 Modified MOV Model

From the literature, it is found that a disc type MOV can be modeled by the following equivalent circuit [1].

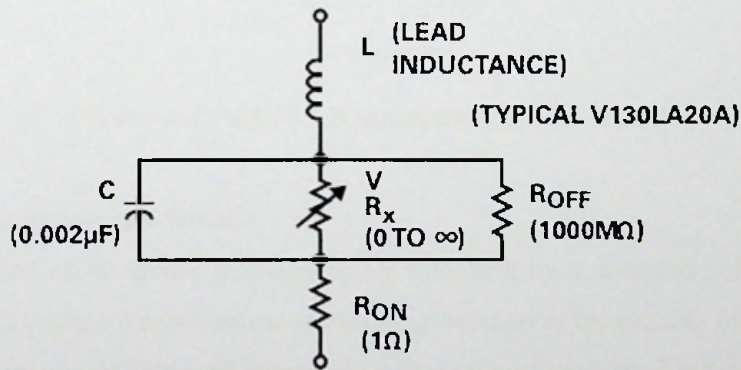


**Figure 4-2: MOV Equivalent Model**

At low currents, the model can be simplified to the following equivalent circuit [1].

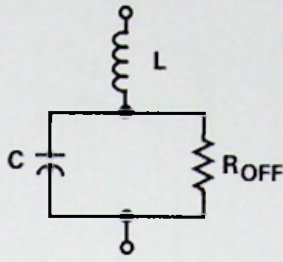


**Figure 4-3: MOV Equivalent Circuit at Low Currents**

The MOV model available in MATLAB has neither a capacitive component nor an inductive component. Therefore, to make the MATLAB model more realistic, the parallel capacitance with the Resistance is added. The value of the capacitance is obtained by measurement. The average value of capacitance for the selected samples is  $560\mu\text{F}$ . The value of lead inductance is considered negligible.

The final version of the model used in the simulation is shown below.

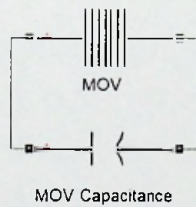


**Figure 4-4: MATLAB Simulation Model of MOV**

#### 4.2.4 Simulation and Results

The modified MOV model is simulated by feeding it by a distorted voltage source. Current and voltage measurements are taken in addition to the plotting of waveforms. Due to the reason, of distorted current and voltage waveforms, the RMS value is taken as the measurement. Both resistive and capacitive current components of the leakage current is measured during the simulation since it is readily available. The block diagram is shown below as figure 4-5.



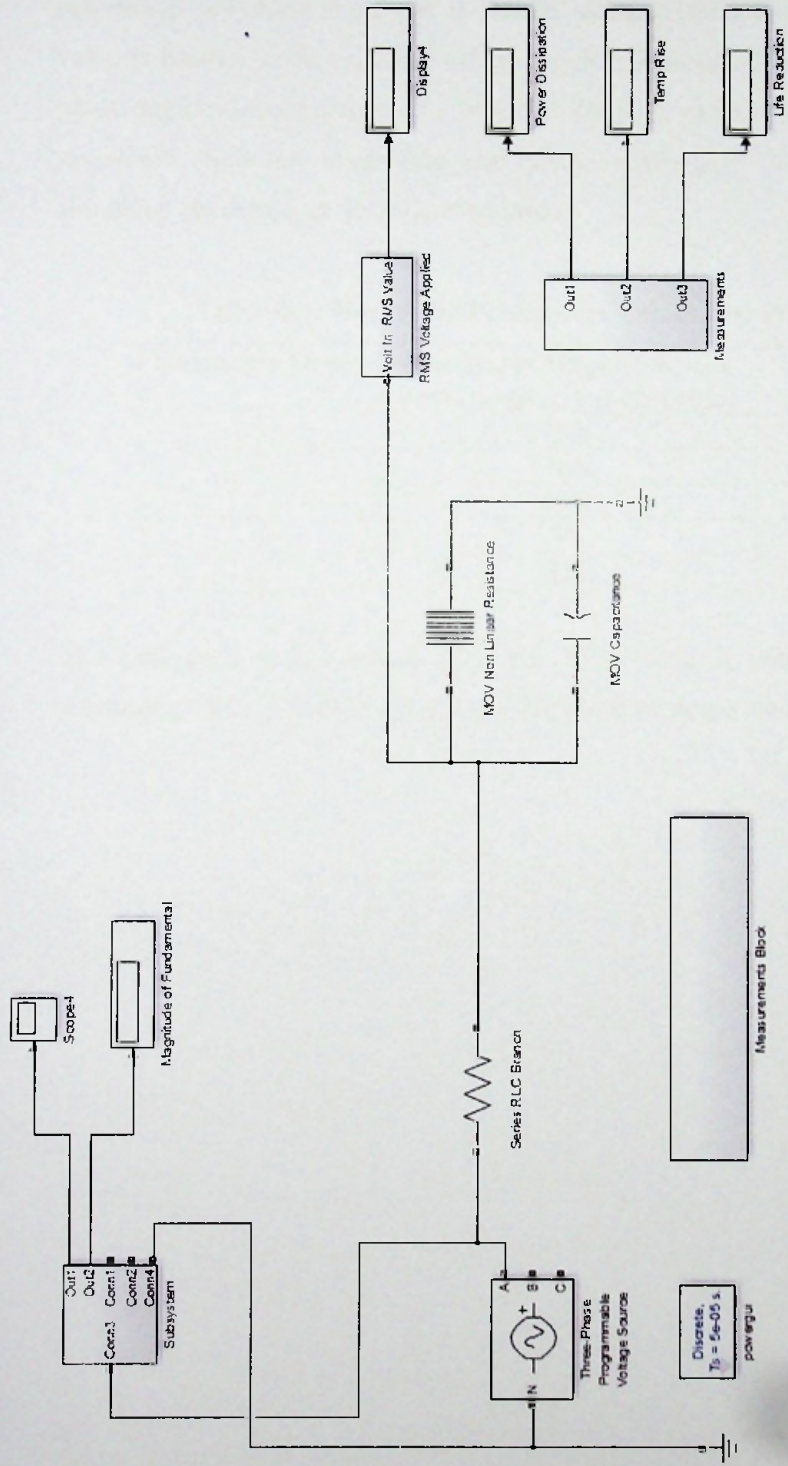


Figure 4-5: Simulation Block Diagram in MATLAB Simulink

When adding harmonics on top of the fundamental to distort the waveform, the magnitude and phase angle has an infinite number of combinations. The magnitude value is limited to the practical values depending on the order of the harmonic. The phase angle is selected in such a way that the peak value of the final waveform is a maximum. Selected magnitude and phase angle pairs for different harmonics simulated are shown in the following table.

**Table 4-3: Harmonic Percentage Values and Phase Angles**

<b>Harmonic Order</b>	<b>Maximum Magnitude as a percentage of fundamental</b>	<b>Phase Angle</b>
3	30%	180
5	20%	0
7	10%	180
9	5%	0
11	5%	180

The base case of the simulation is the MOV feeding with a sinusoidal voltage waveform. The results of the base case are given in figure 4-6 below.



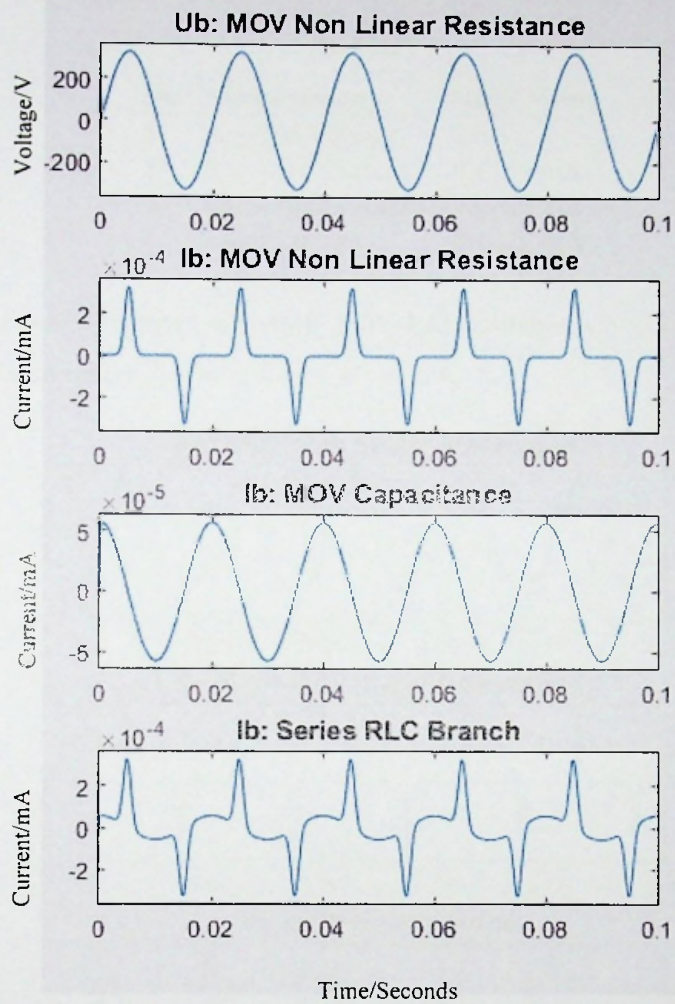


**Figure 4-6: Applied Voltage ( $U_b$ ), Resistive Current Component through MOV ( $I_b$ : MOV nonlinear Resistance), Capacitive Current Component through MOV ( $I_b$ : MOV Capacitance), and Total Current through MOV ( $I_b$ : Series RLC Branch)**

The RMS values of the simulated voltage and currents are as below table 4-4.

**Table 4-4: Simulation Measurements When Pure Sinusoidal Waveform Applied to MOV**

No	Measurement	RMS Value
1	Applied Voltage	230V
2	Resistive Current	0.1169 mA
3	Capacitive Current	0.0405 mA
4	Total Current	0.1239 mA

An example measurement made with 230V RMS voltage waveform distorted with 20% of 5<sup>th</sup> harmonic is shown in figure 4-7 below.

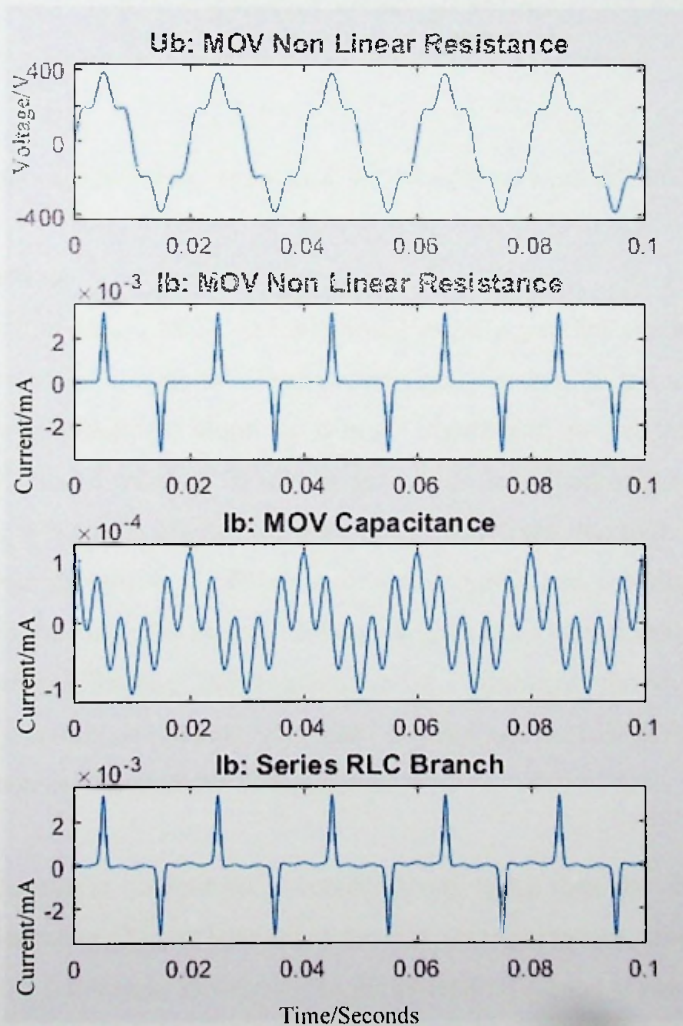


**Figure 4-7: Applied Voltage ( $U_b$ ), Resistive Current Component through MOV ( $I_b$ : MOV nonlinear Resistance), Capacitive Current Component through MOV**



**(I<sub>b</sub>: MOV Capacitance), and Total Current through MOV (I<sub>b</sub>: Series RLC Branch)**

The RMS values of the simulated voltage and currents are given below table 4-5.

**Table 4-5: Simulation Measurements When 5<sup>th</sup> Harmonic 20% Distorted Waveform Applied to MOV**

No	Measurement	RMS Value
1	Applied Voltage	230V
2	Resistive Current	0.8396 mA
3	Capacitive Current	0.0561 mA
4	Total Current	0.8423 mA

Several number of simulation runs were done. Results are available in Appendix II.

#### 4.2.5 Discussion

In this simulation study, MOV is represented using a parallel amalgamation of a nonlinear resistor and a capacitor. Temperature dependence of the nonlinear resistor is not taken into consideration assuming it is not significant. As per the observations made, the behavior of resistive current component is dependent on the instantaneous voltage of the waveform. Higher the peak of the waveform, the higher the resistive current is. Even though the RMS value of the distorted and non-distorted voltage waveforms are the same, the resistive leakage current has a significant difference due to the peak value difference. The resistive heating effect inside the MOV core is due to this resistive current component. Therefore, the heating effect of MOV can be higher when the voltage is distorted due to harmonics.

The capacitive current component is comparatively lesser than the resistive current component. Therefore, its contribution to the total leakage current through the device is less. With the frequency, an increase in the capacitive current is observed and it is since capacitive reactance is inversely relative to the frequency. The variation of resistive and capacitive currents for different cases of simulation is shown in the following figure.

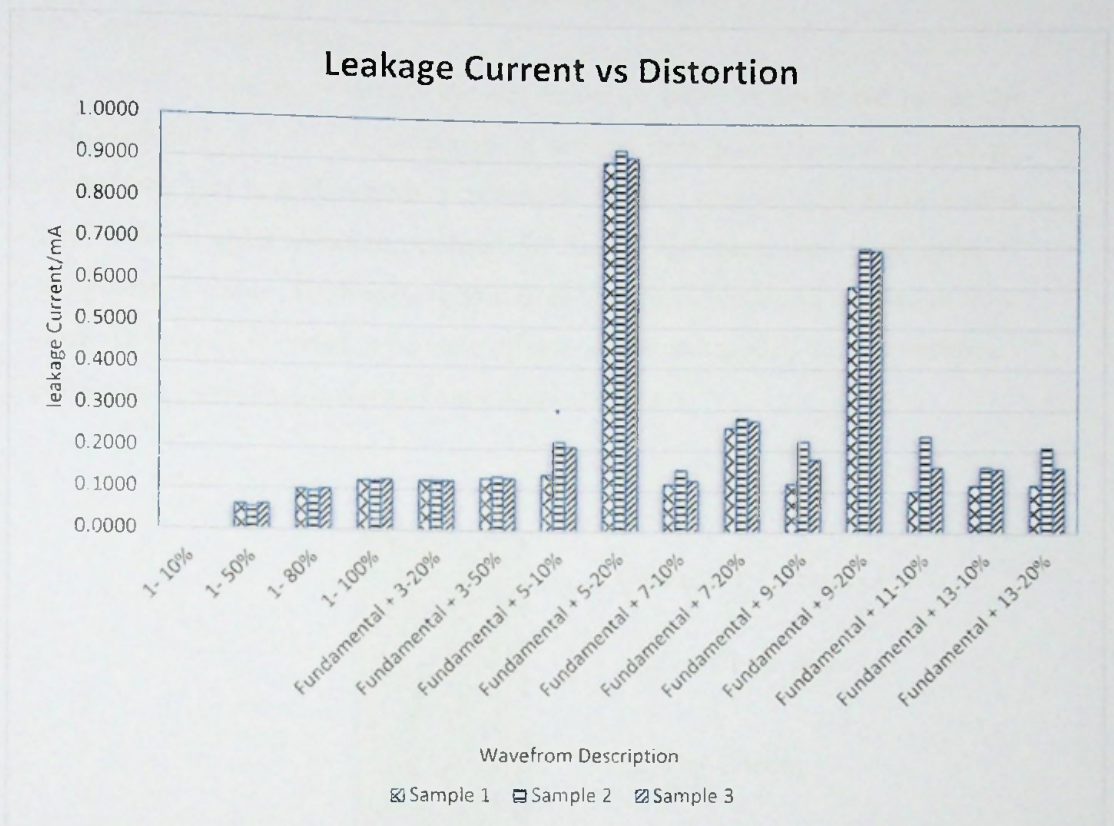


**Figure 4-8: Leakage currents for different levels of distortion (I: Total leakage, Ir: Resistive component and Ic: Capacitive Component)**

When examining the above charts, it is clear that in almost all the cases, the leakage current is high in the distorted scenarios though the RMS value of supply voltage waveform is the same 230V. Higher resistive leakage current will result in premature failure for the MOV.

If the case of distortion with 3<sup>rd</sup> harmonic 30%, the rise of resistive current compared to non-distorted case is approximately 20 times. That is analogous to the rise in power dissipation of 20 times. At no circumstance, this level of leakage current is acceptable. In practice, persistent resistive leakage current more than 1mA is not acceptable. In the long term, persistent leakage current of more than 0.5mA is harmful to the MOV.



### 4.3 MOV Modelling in Thermal Domain (Steady State)

#### 4.3.1 ANSYS Simulation

Using ANSYS software, a simple thermal model of MOV is developed to see the thermal behavior of MOV under persistent internal heat generation due to leakage current. Body part of a 20mm MOV is modeled and its core is set as a heat source where uniform heat generation occurred. In Ansys, heat generation is accepted as Watts per unit volume. The heat generated from the experimental and simulation work carried above was converted to per unit volume values and applied to the simulation. Details of the simulation is shown below figure 4-8 [1].

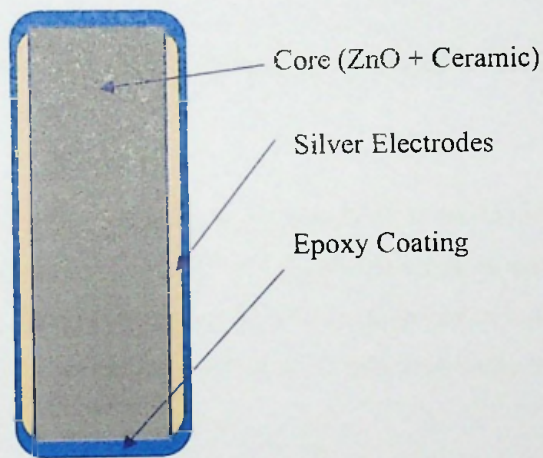


**Figure 4-9: Cross Section of the Modelled MOV**

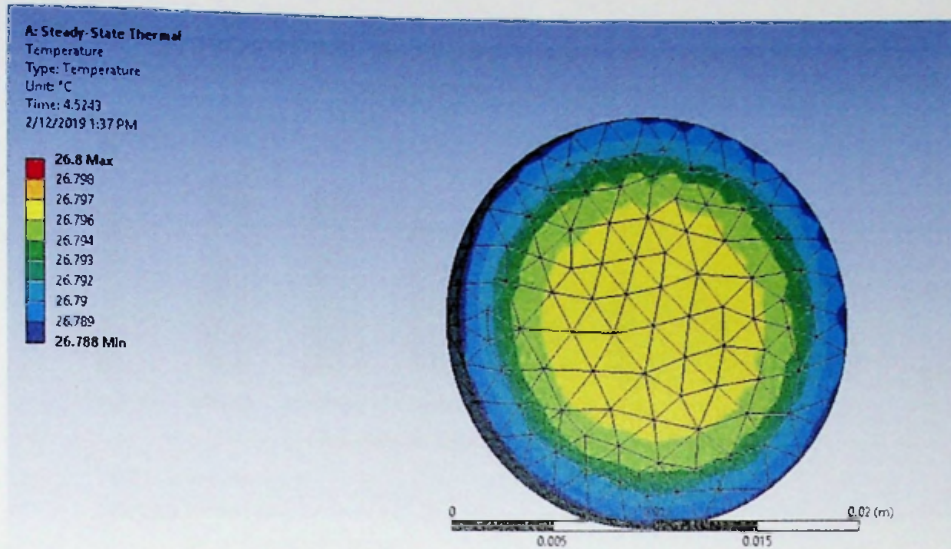


**Figure 4-10: Temperature Distribution of MOV Model in ANSYS**

Ambient temperature was set to 25°C. The cooling of the MOV is due to the convection and radiation mainly. The effect of conduction through the leads is assumed to be negligible. The film coefficient and surface emissivity are adjusted to tune the model with measurement data. Film Coefficient: 25W/m<sup>2</sup> °C and Emissivity 0.95 resulted in the best fit of measured data with simulations.



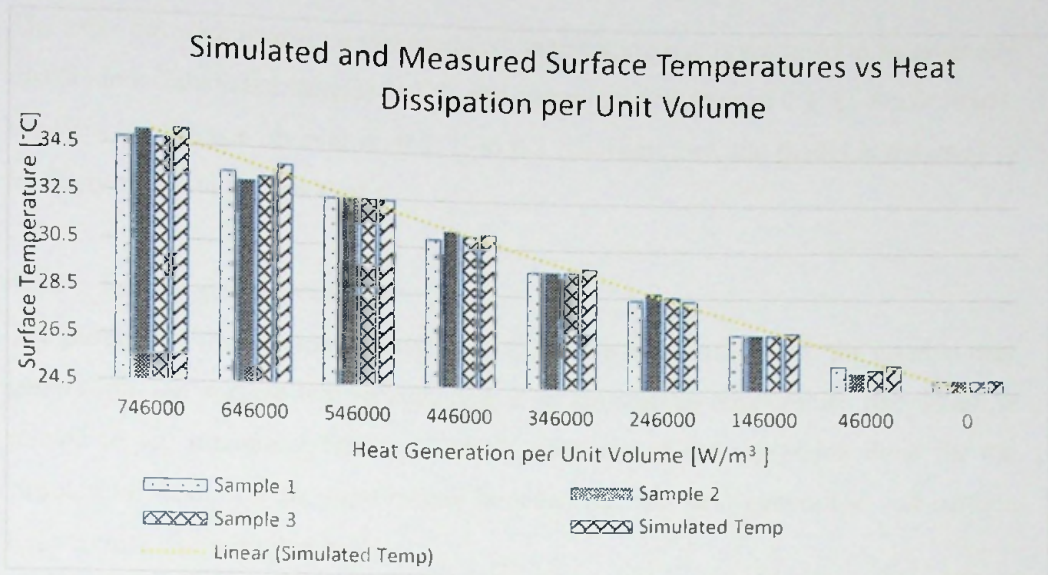


Figure 4-7: Simulated and Measured Surface Temperatures vs Heat Dissipation per Unit Volume

#### 4.3.2 Model Validation

Table 4-6: Simulated and measured temperature data

Dissipation (W)	Dissipation per unit volume (W/m³)	Sample 1 Temperature in °C	Sample 2 Temperature in °C	Sample 3 Temperature in °C	Simulated Temp in °C	Measured Average temperature in °C	Error in °C
0.373	746000	34.8	35.1	34.8	35.2	34.9	-0.3
0.323	646000	33.5	33.1	33.3	33.8	33.3	-0.6
0.273	546000	32.5	32.5	32.5	32.5	32.5	0.0
0.223	446000	30.9	31.2	31.0	31.1	31.0	-0.1
0.173	346000	29.5	29.5	29.5	29.7	29.5	-0.2
0.123	246000	28.4	28.7	28.6	28.4	28.6	0.2
0.073	146000	26.9	26.9	26.9	27.0	26.9	-0.1
0.023	46000	25.6	25.3	25.5	25.6	25.5	-0.2
0	0	25.0	25.0	25.0	25.0	25.0	0.0
						Standard Deviation	0.2
						Mean	-0.1



The error between measured and modeled temperature rise is assumed to be normally distributed. Calculated mean is  $-0.1\text{ }^{\circ}\text{C}$  and a standard deviation of  $0.2\text{ }^{\circ}\text{C}$ . Accordingly, the 95% confidence interval is  $-0.5\text{ }^{\circ}\text{C}$  to  $0.3\text{ }^{\circ}\text{C}$ . Therefore, the model is assumed to be fairly accurate for this study.

### 4.3.3 Results and Discussion

The purpose of this thermal simulation is to build a relationship with the internal heat generation and surface temperature rise. It is the surface temperature rise which is related to the premature failure of MOV. Results of the regression done for the simulation results for the relationship between internal heat generation and surface temperature rise is shown below.

SUMMARY  
OUTPUT

<i>Regression Statistics</i>	
Multiple R	0.99999
R Square	0.99999
Adjusted R Square	0.99999
Standard Error	0.00638
Observations	9

ANOVA					
	<i>df</i>	<i>SS</i>	<i>MS</i>	<i>F</i>	<i>Significance F</i>
Regression	1	103.09142	103.09142	25290.01	1.02671E-20
Residual	7	0.0002853	4.08E-05		
Total	8	103.09170			

	<i>Coefficients</i>	<i>Standard Error</i>	<i>t Stat</i>	<i>P-value</i>	<i>Lower 95%</i>	<i>Upper 95%</i>	<i>Lower 95.0%</i>	<i>Upper 95.0%</i>
Intercept	25.01428	0.004077739	6134.35	8.08E-25	25.00463388	25.02392	25.00463	25.02392
X Variable 1	1.37E-05	8.5955E-09	1590.283	1.03E-20	1.3649E-05	1.37E-05	1.36E-05	1.37E-05

From the regression, the following model is derived for simplification of calculation of temperature rise related to a particular heat dissipation inside MOV.



*Surface Temperature Rise*

$$= 25.01 + 1.37 \times 10^{-5} \times \text{Heat Generation per Unit Volume}$$

From the regression analysis, it is clear that the surface temperature rise has a direct linear relationship with the internal heat generation per unit volume. This equation will be used to calculate the temperature rise of MOV, by using measured or simulated power dissipation of MOV.

## 5. ESTIMATION OF EFFECT OF SUPPLY VOLTAGE DISTORTION ON LIFETIME OF MOV

### 5.1 Introduction

In this chapter, the experimental and simulation work carried out is utilized to estimate the effect of supply voltage distortion on the lifetime expectancy of MOVs. Using the results of the experiments, the thermal and electrical models are verified. Using the electrical mode, the resistive leakage current and power dissipation of the MOV is obtained.

This power dissipation value is fed into the thermal model to calculate the temperature rise. The temperature rise value is used to evaluate the life expectancy using, life expectancy models available in the literature.

### 5.2 Lifetime Estimation Model

In literature, no life expectancy estimation models are found for MOVs relating to their body temperature. The well-known Arrhenius equation has widely been used for accelerated lifetime testing. The standard IEEE C62.11-2012 [9], IEEE Standard for Metal-Oxide Surge Arresters for AC Power Circuits (>1 kV) has the following information on accelerated life testing.

*Basis for accelerated aging procedure*

*Based on Arrhenius life tests of metal-oxide block designs that increase in power loss with time, the following statements apply:*

*40 °C is a conservative weighted average use temperature for all arresters except liquid-immersed and deadfront arresters.*

*The block aging process is accelerated by elevated temperature.*



The temperature acceleration rate is reasonably estimated by an acceleration factor  $A_{FT}$ .

Where

$$A_{FT} = 2.5^{(\Delta T) / (10)}$$

Where

$\Delta T$  is the difference between test temperature and weighted average use temperature"

It is understood that the above information in the standard refers to the arrestor operation in an elevated temperature environment. This research discusses about the arrestor operation in nominal ambient temperature with an elevated body temperature. It is assumed that the effect on the life expectancy of MOV is same for the both of the above cases namely operating in elevated ambient temperature and operating in nominal ambient temperature with a higher body temperature.

Hence,  $1/A_{FT}$  is equal to the expected life span ratio of the MOV as per the following equation

$$\text{Life at Elevated Temperature} = \text{Life at Nominal Temperature} / A_{FT}$$

The  $1/A_{FT}$  calculation for different distortion scenarios is shown in the results below table 5-1.

### 5.3 Results

**Table 5-1: Results of Lifetime Estimation for Different Levels of Distortion**

Scenario	Power Dissipation [W]	Temp Rise ( $\Delta T$ ) [ $^{\circ}$ C]	Expected Lifetime from 40 Degrees Lifetime ( $1/A_{FT}$ )
<b>Fundamental</b>	0.000	0.0	1.00
<b>Fund + 3rd 30%</b>	0.393	10.8	0.37
<b>Fund + 5th 20%</b>	0.100	2.7	0.78
<b>Fund + 7th 10%</b>	0.040	1.1	0.90

Fund + 9th 5%	0.020	0.6	0.95
Fund + 11th 5%	0.020	0.6	0.95
Fund + 13th 5%	0.019	0.5	0.95
Fund + 15th 5%	0.016	0.5	0.96
Fund +3rd 20% + 5th 10%	0.460	12.6	0.32
Fund +3rd 20% + 7th 10%	0.390	10.7	0.38
Fund +5th 20% + 7th 10%	0.320	8.8	0.45

#### 5.4 Discussion

As per the results, harmonic distortion is a reason for the reduction of the lifetime of MOV. In some cases, the life expectancy is as low as 32% while some causes not impose significant reductions. The expected lifetime together with the peak value of the applied voltage waveform is shown below figure 5-1 to identify the reason for life expectation reduction.



**Figure 5-1: Per unit life expectancy with a peak value of Voltage waveform for different levels of distortion**



As per the above chart, it is clear that the life expectation reduces when the peak of the waveform is higher than the peak of the non-distorted case. The higher the peak is the lesser is the anticipated life span is. But for the last three waveforms, it is evident that life expectancy is different even though the peak is the same. The explanation is provided using the following chart.

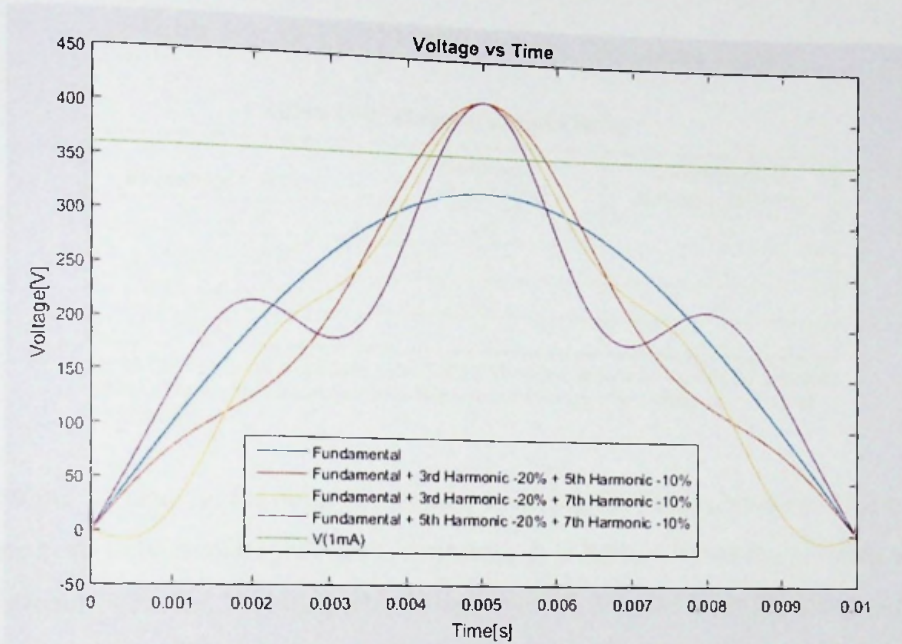


**Figure 5-2: Behavior of Peak Value of the waveform for different level of distortions for the same RMS value**

The chart above contains fundamental and three different distorted waveforms with the given harmonics in the legend. Their RMS value is the same and the peak is the same. The line  $V_{1mA}$  shows the MOVs voltage at 1mA current. Whenever the voltage rises above this line, the current flowing through MOV increases drastically for keeping the Voltage from rising. Whenever the area between input waveform and the  $V_{1mA}$  line is higher compared to the waveform with the same peak, the current flowing is also high.

When more current is flowing through MOV, there will be more dissipation of power. That excess power dissipation is a reason for the body temperature of MOV to rise. Operation at elevated body temperature is the reason for premature failure.



IEEE 519-2014 [2] is the standard which laid limits to the voltage total harmonic distortion for utility supply voltages. The following table shows the applicable limits.

**Table 5-2: IEEE-519-2014 Voltage Distortion Limits**

**Table 1—Voltage distortion limits**

Bus voltage $V$ at PCC	Individual harmonic (%)	Total harmonic distortion THD (%)
$V \leq 1.0 \text{ kV}$	5.0	8.0
$1 \text{ kV} < V \leq 69 \text{ kV}$	3.0	5.0
$69 \text{ kV} < V \leq 161 \text{ kV}$	1.5	2.5
$161 \text{ kV} < V$	1.0	1.5 <sup>1</sup>

<sup>1</sup>High-voltage systems can have up to 2.0% THD where the cause is an HVDC terminal whose effects will have attenuated at points in the network where future users may be connected.

As per the standard, at the point of common coupling (PCC) the above maximum THD values need to be maintained. For LV systems, it is 8.0%. One of the possible worst-case scenarios in the LV system with distortion of 3<sup>rd</sup>, 5<sup>th</sup> and 7<sup>th</sup> harmonics considered. To have a THD of 8% following individual components used.

**Table 5-3: Composition of Harmonics for 8% THD**

Harmonic	Percentage	Angle
3rd	5%	180
5th	5%	0
7th	3.7%	180
THD	8%	



The results of the simulation are as below figure 5-3.

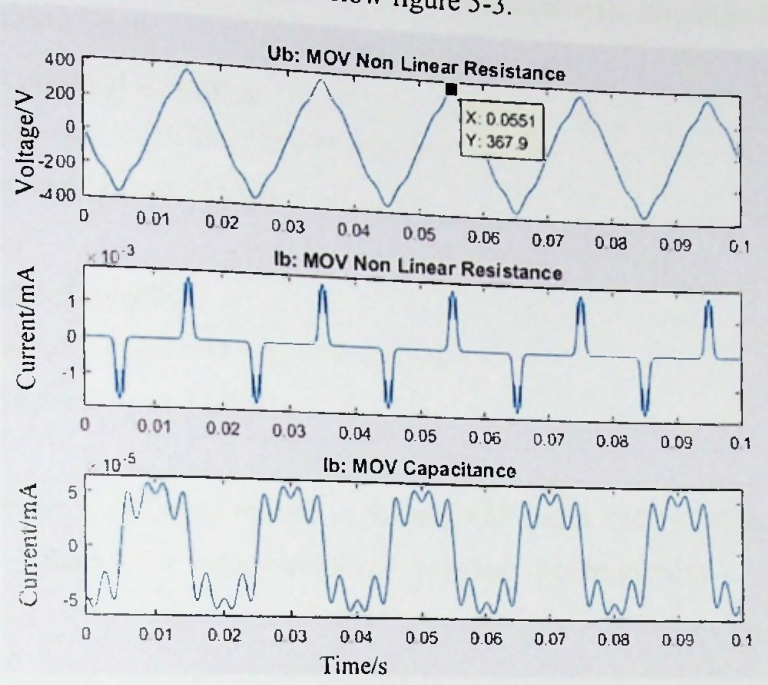


**Figure 5-3: Results for 8% THD in Voltage**

Resistive Leakage Current: 0.52 mA

Power Dissipation: 0.07W

Temperature Rise: 2 Degrees Celsius

Expected Life: 76% from Rated Life

The implied result is that even under the accepted distortion limit, the selected MOV type is going to suffer a 24% reduction in life in the assumed case. Therefore, selecting the MCOV of MOSA is a critical decision that needs to be taken considering the effect of harmonics.

The increased dissipation in the devices can increase the total power loss in the system significantly. Depending on the MCOV of the device and peak value of the supply voltage waveform, power loss is going to be increased. This value needs to be calculated for each device separately because of the nonlinear behavior of MOVs.

If the tested types of MOVs are available in a transformer area of 250 homes, 5 in each home inside different appliances. Let's consider a worst-case distortion level under IEEE-519-2014 limits.

Under non distorted conditions

$$\text{Power dissipation} = 0.018\text{W} * 250 * 5 = 22.5\text{W}$$

$$\text{Energy loss per day} = 0.54 \text{ kWh}$$

Under distorted conditions

$$\text{Power dissipation} = 0.070\text{W} * 250 * 5 = 87.5\text{W}$$

$$\text{Energy loss per day} = 2.1 \text{ kWh}$$

$$\text{Percentage rise in power dissipation in the area} = 87.5/22.5 * 100 = 388\%$$

By selecting the MCOV value carefully, this situation can be avoided.



**6. DISCUSSION****6.1 Introduction**

In this chapter, a discussion is presented about the findings of this research work followed by a comparison with the available literature. Further, the validity of the results obtained are discussed and the feasibility of applying them for MV surge arrestors made from MOV discs.

**6.2 Results in Contrast with Literature**

Both of the simulation studies and experiments performed revealed that distorted voltage waveforms applied to MOV surge arrestors can increase the steady-state power dissipation. The reason behind this possibility is identified as the peak voltage rise of the voltage waveform due to the harmonics. Some combinations of harmonic order and phase angles increase the peak of the waveform when added on the fundamental.

Due to the increased power dissipation, MOVs will stay hotter throughout their operational life which will be a reason for premature failure. By nature, MOVs are capable of dissipating energy of transients which are very short in duration. A tradeoff of increased clamping voltage is experienced every time the MOV dissipated energy of a surge. This behavior makes the device useless after a certain number of strokes since it loses the capability of providing the required level of protection to the downstream.

Experiments performed followed with model validation for simulation in electrical and thermal domains. The adverse effect of operation at elevated body temperature was quantified using the equation presented in IEEE C62.11-2012 [9] standard.

Eda, Iga, and Matusoka [3] have concluded from their work that, the amount of leakage current, as well as the temperature, has a direct impact on the life expectancy of MOVs.

Zhou, Zhang, and Gong [4] studied the degradation phenomena of low voltage ZnO varistors caused by dc biasing at elevated temperatures. They have found that due to temperature and DC bias V-I characteristics of MOVs degrade increasing the clamping voltage. The work presented in this thesis has strengthened the above findings and, in the meantime, gone further by quantifying the adverse effect on lifetime.

D. Kladar, F. Martzloff and D. Natasi [5] have discussed TOV effects on surge-protective devices. Since the TOV on SPD implies the increased leakage current, the expected results are as same as the above literature and findings of this research.

Yuanfang Wen and Chengke Zhou [6] present a methodology for predicting the lifetime of metal-oxide varistor (MOV), which is a cumbersome method involve a large number of experiments. Therefore, the practical use of the method is highly limited. The method used in this research is simple and in line with the IEEE standard. Therefore, it is envisaged that this work can be more useful in the phase of design.

### **6.3 Limitations and Applicability for Utility-Scale MV Applications**

The work carried out under this research was conducted for LV MOVs. The results derived are applicable mostly for the LV rated MOVs used in electronic devices. When it comes to utility applications, LV MOSAs are rarely used. Medium Voltage systems always are protected using MV rated MOSAs usually at primary substations, distribution substations and other related switchgear like load break switches.

These MOSAs are made using a stack of MOV discs encapsulated in a suitable housing structure [20]. The resultant device has thermal and electrical behavior deviated from the MOVs used for LV applications. The resistive leakage current of the MOSA is expected not to have heavily deviated from the characteristics of MOV. Yet, the capacitive component of the current will be heavily changed due to the additional capacitive effects of the construction.

Therefore, the derivations of this work need farther refinement for directly applying for MV rated MOSAs.



## 7. CONCLUSIONS AND RECOMMENDATIONS

This study reveals that the presence of harmonics can become a reason for premature failure of MOV and hence the MOSAs. When harmonics are present with specific magnitude and phase angle combinations can be a reason to increase the peak voltage of the waveform higher than the peak voltage of the non-distorted voltage waveform. The peak value of the waveform has a direct relationship with Resistive leakage current through the MOV. The higher the peak voltage, the higher will be the resistive leakage current and the power dissipation.

Therefore, when selecting MCOV of the MOSA, attention should be paid about the possible maximum system peak voltage. It is better to consider the effect of harmonics on the maximum voltage on top of the other factors. It is not the RMS value of the voltage, but the factor governing the magnitude of the leakage current is the peak value of the waveform.

Another important factor for increased leakage current is the shape of the waveform. When the waveform is wider near the peak, RMS leakage current increases. Operating a MOV at continuous excess power dissipation can shorten the lifetime of the MOV. As per the IEEE C62.11-2012 [9] standard-based calculations, the loss of life expectancy can become significant in some situations.

### 7.1 Recommendations

To minimize this problem following recommendations are made assuming that system voltage distortion is maintained under the limits of IEEE-519-2014.

**Table 7-1: Recommended MCOV Values**

Bus Voltage at PCC	Individual Harmonic %	THD (%)	Max Possible Voltage Peak When Distorted (%) (considering 3 <sup>rd</sup> , 5 <sup>th</sup> & 7 <sup>th</sup> Harmonics)	CEB Specified MCOV (Min)(RMS)	MCOV as Per IEEE C62.11-2012	Recommended Minimum Value of MCOV (RMS)
$V \leq 1.0\text{kV}$	5	8	113%	NA	NA	400V System: 390V
$1\text{kV} < V \leq 69\text{kV}$	3	5	108%	11kV System (Max 12kV) - 9.6kV	10.2kV	11kV System (Max 12kV) - 11.0 kV
				33kV System (Max 36 kV) - 28.8kV	29kV	33kV System (Max 36kV) - 31.3 kV
$69\text{kV} < V \leq 161\text{kV}$	1.5	2.5	104%	132kV System (Max 145kV): NA	115kV	132kV System (Max 145kV): 119.6 kV
$161\text{kV} < V$	1	1.5	102%	220kV System (Max 245 kV): NA	190kV	220kV System (Max 245 kV): 193.8 kV

As shown in row number 1, for LV systems, it is recommended to use MCOV values above 390V for Line to Neutral applications. The basis for the selected value is the RMS value of line to neutral voltage multiplied by 1.5 factor from C62.11-2012 [9] standard and by 1.13 factor from IEEE-519-2014 as shown in the table.

Likewise, for  $1\text{kV} < V \leq 69\text{kV}$  category CEB has 11kV delta and 33V delta systems. It is recommended to use MCOV of 11kV in 11kV systems and 31.3kV in 33kV systems when selecting MOSAs. It is noted that the values used by CEB is not sufficient in the scenarios where harmonic overvoltages.

For  $69\text{kV} < V \leq 161\text{kV}$  range, CEB's applications are on 132kV. The suggested value of MCOV in IEEE C62.11-2012 [9] is 115kV. It is proposed to increase this value by 1.04 to match with the possible peak voltage due to distortion. The resultant value is 119.6kV.





## 7.2 Study Limitations and Suggestions for Future Work

MOVs are under LV conditions tested in this study to assess the effect of supply voltage harmonics on MOSAs due to the reason for the unavailability of MV/HV test equipment and MV/HV harmonic sources. Thus, an avenue is available to extend the experiments to MV/HV levels with real MOSAs but not MOVs.

Further, the behavior of leakage current against the time when exposed to distorted voltages is not considered in this work. The failure point of a MOV can be precisely detected by the magnitude of resistive leakage current when passing a certain limit. Therefore, if the leakage current can be logged continuously to fit a model against time, then it will reveal whether the failure occurs before the catastrophic failure or Arrhenius life estimation.

## 8. REFERENCES

- [1] Littelfuse.com. (2018). [online] Available at: [http://www.littelfuse.com/~media/electronics/product\\_catalogs/littelfuse\\_varistor\\_catalog.pdf](http://www.littelfuse.com/~media/electronics/product_catalogs/littelfuse_varistor_catalog.pdf) [Accessed 4 Jun. 2018].
- [2] IEEE 519-2014 - IEEE Recommended Practice and Requirements for Harmonic Control in Electric Power Systems.
- [3] K. Eda, A. Iga, and M. Matsuoka. Degradation mechanism of non-ohmic zinc oxide ceramics. *Journal of Applied Physics*, 1(5):2678-2684, January 1980.
- [4] D.Zhou, C.Zhang, and S.Gong. Degradation phenomena due to dc bias in low voltage ZnO varistors. *Materials Science and Engineering: B*, 1-3(99):412-415, May 2003.
- [5] D. Kladar, F. Martzloff and D. Natasi. TOV Effects on Surge-Protective Devices. *Power Quality Exhibition and Conference, Baltimore*, October 25-27 2005.
- [6] Y. Wen and C. Zhou. A Novel Method for Predicting the Lifetime of MOV. *IEEE transactions on power delivery*, vol. 19, no. 4, October 2004.
- [7] M.Jaroszewski, P. Kostyla, and K. Wiczorek. Effect of voltage harmonics content on arrester diagnostic result. *Proceedings of the International Conference on Solid Dielectrics (ICSD 2004), Toulouse, France*, July 2004.
- [8] Technical note on Capacitor lifetime. Rubicon Corporation. [[www.rubycon.co.jp/en/products/alumi/pdf/Life.pdf](http://www.rubycon.co.jp/en/products/alumi/pdf/Life.pdf)].
- [9] IEEE Std C62.11-2012 IEEE Standard for Metal-Oxide Surge Arresters for AC Power Circuits (>1 kV).
- [10] M. Balci and M. Hocaoglu. On the validity of harmonic source detection methods and indices. *Proceedings of the 14th International Conference on Harmonics and Quality of Power, Bergamo, Italy*, September 2010.
- [11] R. Herrera, P. Salmeron, and S. Litran. Assessment of harmonic distortion sources in power networks with capacitor banks. *Proceedings of the 11th International Conference on Renewable Energies and Power Quality, Las Palmas de Gran Canary, Spain*, April 2011.
- [12] C.de Salles, M. L. Martinez, and A.A. de Queiroz. Ageing of metal oxide varistors due to surges. *Proceedings of the International Symposium on Lightning Protection (XI SIPDA), Fortaleza, Brazil*, October 2011.



- [13] R.A. Sargent, G. L. Dunlop, and M. Darveniza. Effects of multiple impulse currents on the microstructure and electrical properties of metal oxide varistors. *IEEE Transactions on Electrical Insulation*, 6(3):586-592, June 1992.
- [14] P.Osmokrovic, B. Loncar, S. Stankovic, and S.Vasic. Aging of the over-voltage protection elements caused by over-voltages. *Microelectronics Reliability*, 12(12): 1959 -1966, December 2002.
- [15] C.Nahm. Pulse aging behavior of ZnO-pr6o11-coo-cr2o3-dy2o3 varistor ceramics with sintering time. *Ceramics international*, 37(6):1409{1414, May 2011.
- [16] W. Sun, Y. Li, D. Zeng, R. Cai, and Z. Meng G. Yang. Investigation of voltage current characteristics of ZnO varistors under 8/20 microsecond impulse current. *The IEEE Power Engineering and Automation Conference, Wuhan, China*, September 2011.
- [17] C. Karawita and M.Raghuveer. Leakage current based assessment of degradation of MOSA using an alternative technique. *Annual Report of the Conference on Electrical Insulation and Dielectric Phenomena (CEIDP'05)*, pages 199-201, October 2005
- [18] J. He, R. Zeng, Y. Tu, S. Han, and H. Cho. Aging characteristics and mechanisms of ZnO nonlinear varistors. *Proceedings of the 6th International Conference on Properties and Applications of Dielectric Materials, Xi'an, China*, June 2000.
- [19] MATLAB Simulink Documentation. (2019). [online] Available at: <https://www.mathworks.com/help/simulink/> [Accessed 4 Jun. 2019].
- [20] Medium-voltage surge arresters production video (smaller format). (2019). [video] Available at: <https://search-ext.abb.com/library/Download.aspx?DocumentID=9AKK107046A9495&LanguageCode=en&DocumentPartId=Lower%20resolution&Action=Launch> [Accessed 19 Nov. 2019].
- [21] V.P. Rabde. Metal oxide varistors as surge suppressors. *Proceedings of the 1995 International Conference on Electromagnetic Interference and Compatibility (INCEMIC)*, Madras, India.

**Appendix I**  
**Results of the Electrical Experiments Performed**

Voltage	Sample 1	Sample 2	Sample 3	I - Simulation	diff	Error %
Fundamental - 10%	0.0000	0.0000	0.0000	0.0132	-0.0044	
Fundamental - 50%	0.0614	0.0560	0.0623	0.0662	0.0011	1.7
Fundamental - 80%	0.0989	0.0960	0.1006	0.1059	0.0003	0.3
Fundamental - 100%	0.1224	0.1220	0.1244	0.1416	-0.0043	-3.0
Fundamental + 3-20%	0.1231	0.1231	0.1231	0.1235	-0.0001	-0.1
Fundamental + 3-50%	0.1281	0.1321	0.1291	0.1335	-0.0021	-1.6
Fundamental + 5-10%	0.1378	0.2188	0.2058	0.2740	-0.0044	-1.6
Fundamental + 5-20%	0.9023	0.9333	0.9143	0.8701	0.0124	1.4
Fundamental + 7-10%	0.1166	0.1526	0.1256	0.1505	-0.0143	-9.5
Fundamental + 7-20%	0.2563	0.2813	0.2733	0.3008	-0.0062	-2.1
Fundamental + 9-10%	0.1194	0.2234	0.1794	0.2614	-0.0220	-8.4
Fundamental + 9-20%	0.6022	0.6952	0.6912	0.7009	0.0251	3.6
Fundamental + 11-10%	0.1018	0.2368	0.1608	0.2014	-0.0192	-9.5
Fundamental + 13-10%	0.1166	0.1616	0.1576	0.1705	0.0080	4.7
Fundamental + 13-20%	0.1182	0.2092	0.1592	0.2008	-0.0169	-8.4



## Appendix II

### Results of the Simulations Performed

#### CASE 2 – 3<sup>RD</sup> HARMONIC DISTORTION

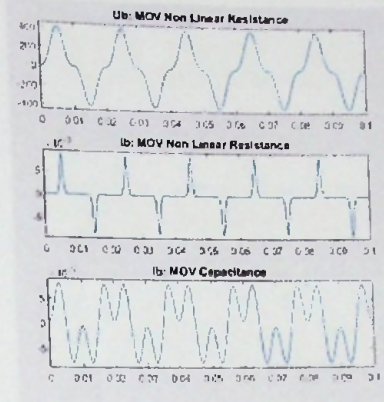
Fundamental + 30 % 3<sup>rd</sup> Harmonic  
Harmonic Phase Angle: 180 degrees

Resistive Leakage Current: 2.44mA rms

Power Dissipation: 0.39W

Temperature Rise: 10.8°C

Expected Life : 37% from rated life



#### CASE 2 – 3<sup>RD</sup> HARMONIC DISTORTION

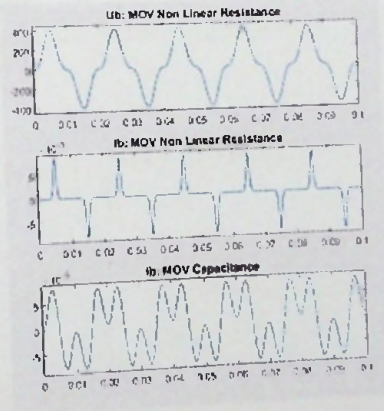
Fundamental + 30 % 3<sup>rd</sup> Harmonic  
Harmonic Phase Angle: 180 degrees

Resistive Leakage Current: 2.44mA rms

Power Dissipation: 0.39W

Temperature Rise: 10.8°C

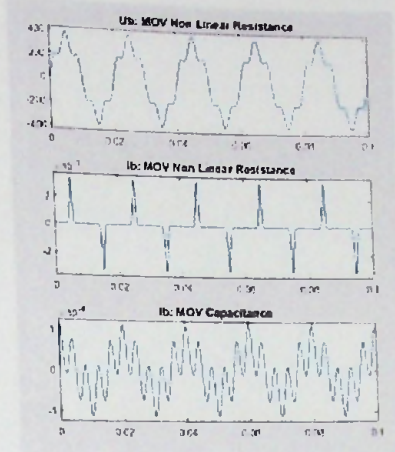
Expected Life : 37% from rated life



## CASE 2 – 5<sup>TH</sup> HARMONIC DISTORTION

Fundamental + 20 % 5<sup>th</sup> Harmonic  
Harmonic Phase Angle: 0 degrees

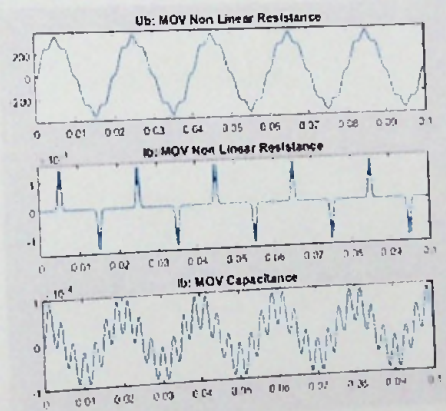
Resistive Leakage Current: 0.41mA rms  
Power Dissipation: 0.10W  
Temperature Rise: 2.8°C  
Expected Life : 78% from rated life



## CASE 3 – 7<sup>TH</sup> HARMONIC DISTORTION

Fundamental + 10 % 7<sup>th</sup> Harmonic  
Harmonic Phase Angle: 180 degrees

Resistive Leakage Current: 0.17mA rms  
Power Dissipation: 0.04W  
Temperature Rise: 1.1°C  
Expected Life : 90% from rated life

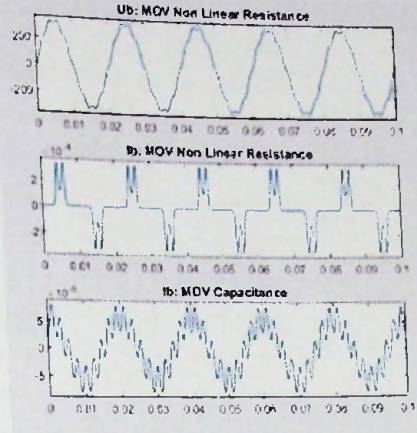




## CASE 4 — 9<sup>TH</sup> HARMONIC DISTORTION

Fundamental + 5 % 9<sup>th</sup> Harmonic  
Harmonic Phase Angle: 0 degrees

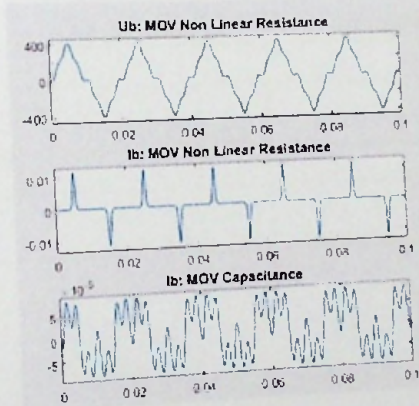
Resistive Leakage Current: 0.12mA  
Power Dissipation: 0.02W  
Temperature Rise: 0.6°C  
Expected Life : 95% from rated life



## FUNDAMENTAL + 3<sup>RD</sup> HARMONIC + 7<sup>TH</sup> HARMONIC

Fundamental  
+ 3<sup>rd</sup> - 20% (180 degrees)  
+ 7<sup>th</sup> - 10% (180 degrees)

Resistive Leakage Current: 2.8mA  
Power Dissipation: 0.39W  
Temperature Rise: 11°C  
Expected Life : 38% from rated life



### Appendix III

#### Measurements of MOV Voltage at 1mA DC Current

Measurement No	Sample 1 Voltage [V]		Sample 2 Voltage [V]		Sample 3 Voltage [V]	
1	371.17					
2	371.42		359.33		357.7	
3	371.55		361.41		357.59	
4	371.62		361.42		357.59	
5	371.65		361.6		357.58	
6	371.62		363.16		357.6	
7	371.63		363.15		357.59	
8	371.82		363.16		357.61	
9	372.05		363.05		357.7	
10	372.07		363.05		357.7	
			363.05		357.79	
Mean	371.66	V	362.238	V	357.645	V
Standard Deviation	0.27076	V	1.279243	V	0.071995	V
Leakage current at 325V	0.168	mA	0.1682	mA	0.17	mA
Temperature rise (degrees Celsius)	10		10		10	



## Appendix IV

### Yokogawa WT310 Measurement Error Analysis

Measurement (mA)	Error ( $\mu$ A)	Measurement (mA)	Error ( $\mu$ A)
0.01	10.01	2.51	12.51
0.06	10.06	2.56	12.56
0.11	10.11	2.61	12.61
0.16	10.16	2.66	12.66
0.21	10.21	2.71	12.71
0.26	10.26	2.76	12.76
0.31	10.31	2.81	12.81
0.36	10.36	2.86	12.86
0.41	10.41	2.91	12.91
0.46	10.46	2.96	12.96
0.51	10.51	3.01	13.01
0.56	10.56	3.06	13.06
0.61	10.61	3.11	13.11
0.66	10.66	3.16	13.16
0.71	10.71	3.21	13.21
0.76	10.76	3.26	13.26
0.81	10.81	3.31	13.31
0.86	10.86	3.36	13.36
0.91	10.91	3.41	13.41
0.96	10.96	3.46	13.46
1.01	11.01	3.51	13.51
1.06	11.06	3.56	13.56
1.11	11.11	3.61	13.61
1.16	11.16	3.66	13.66
1.21	11.21	3.71	13.71
1.26	11.26	3.76	13.76
1.31	11.31	3.81	13.81
1.36	11.36	3.86	13.86
1.41	11.41	3.91	13.91
1.46	11.46	3.96	13.96
1.51	11.51	4.01	14.01
1.56	11.56	4.06	14.06
1.61	11.61	4.11	14.11
1.66	11.66	4.16	14.16
1.71	11.71	4.21	14.21
1.76	11.76	4.26	14.26
1.81	11.81	4.31	14.31
1.86	11.86	4.36	14.36

Measurement (mA)	Error ( $\mu$ A)	Measurement (mA)	Error ( $\mu$ A)
1.91	11.91	4.41	14.41
1.96	11.96	4.46	14.46
2.01	12.01	4.51	14.51
2.06	12.06	4.56	14.56
2.11	12.11	4.61	14.61
2.16	12.16	4.66	14.66
2.21	12.21	4.71	14.71
2.26	12.26	4.76	14.76
2.31	12.31	4.81	14.81
2.36	12.36	4.86	14.86
2.41	12.41	4.91	14.91
2.46	12.46	4.96	14.96
		5.01	15.01

